

Colloquium: Nonlinear collective interactions in quantum plasmas with degenerate electron fluids

P. K. Shukla* and B. Eliasson

RUB International Chair, Fakultät für Physik und Astronomie, Ruhr-Universität Bochum, D-44780 Bochum, Germany

(Received 27 September 2010; published 7 September 2011)

The current understanding of some important nonlinear collective processes in quantum plasmas with degenerate electrons is presented. After reviewing the basic properties of quantum plasmas, model equations (e.g., the quantum hydrodynamic and effective nonlinear Schrödinger-Poisson equations) are presented that describe collective nonlinear phenomena at nanoscales. The effects of the electron degeneracy arise due to Heisenberg's uncertainty principle and Pauli's exclusion principle for overlapping electron wave functions that result in tunneling of electrons and the electron degeneracy pressure. Since electrons are Fermions (spin-1/2 quantum particles), there also appears an electron spin current and a spin force acting on electrons due to the Bohr magnetization. The quantum effects produce new aspects of electrostatic (ES) and electromagnetic (EM) waves in a quantum plasma that are summarized in here. Furthermore, nonlinear features of ES ion waves and electron plasma oscillations are discussed, as well as the trapping of intense EM waves in quantum electron-density cavities. Specifically, simulation studies of the coupled nonlinear Schrödinger and Poisson equations reveal the formation and dynamics of localized ES structures at nanoscales in a quantum plasma. The effect of an external magnetic field on the plasma wave spectra and develop quantum magnetohydrodynamic equations are also discussed. The results are useful for understanding numerous collective phenomena in quantum plasmas, such as those in compact astrophysical objects (e.g., the cores of white dwarf stars and giant planets), as well as in plasma-assisted nanotechnology (e.g., quantum diodes, quantum free-electron lasers, nanophotonics and nanoplasmonics, metallic nanostructures, thin metal films, semiconductor quantum wells, and quantum dots, etc.), and in the next generation of intense laser-solid density plasma interaction experiments relevant for fast ignition in inertial confinement fusion schemes.

DOI: [10.1103/RevModPhys.83.885](https://doi.org/10.1103/RevModPhys.83.885)

PACS numbers: 05.30.Fk, 52.35.Mw, 52.35.Ra, 52.35.Sb

CONTENTS

| | |
|---|-----|
| I. Introduction | 885 |
| II. Basic properties of quantum plasmas | 887 |
| III. Model equations for quantum plasmas | 889 |
| A. The Schrödinger and Wigner-Poisson equations | 890 |
| B. The QHD equations | 891 |
| C. The NLS-Poisson equations | 891 |
| IV. Linear waves in quantum plasmas | 891 |
| A. Electron plasma oscillations | 891 |
| B. Ion plasma oscillations (IPOs) | 892 |
| C. High-frequency EM waves | 893 |
| V. Quantum dark solitons and vortices | 893 |
| A. Quantum electron cavity | 893 |
| B. Quantum electron vortices | 894 |
| VI. Quantum electron fluid turbulence | 895 |
| VII. Nonlinearly coupled EM and ES waves | 897 |
| A. Stimulated scattering instabilities | 897 |
| B. Nonlinearly coupled intense EM and EPOs | 898 |
| VIII. Magnetized quantum plasmas | 900 |
| A. Landau quantization | 900 |
| B. ESOs and EM waves | 901 |
| C. Q-HMHD equations | 902 |
| IX. Summary and outlook | 902 |

I. INTRODUCTION

Dense plasmas composed of ions, degenerate electrons, positrons, and/or holes (in the context of semiconductors) are referred to as quantum plasmas. In the latter, the degeneracy of the lighter plasma species (electrons, positrons, holes) appears at very high densities and relatively low temperatures, where the mean interparticle distance is smaller than (or of the same order as) the de Broglie thermal wavelength. The ions are typically nondegenerate due to their relatively large mass in comparison with the electron mass. In quantum physics, Heisenberg's uncertainty principle (Dirac, 1981; Holland, 1993; Landau and Lifshitz, 1998a; Bransden and Joachain, 2000) dictates that conjugate variables, such as the position and momentum of a particle, cannot be precisely determined simultaneously; the product of the uncertainties of the position and momentum is equal to or larger than $\hbar/2$, where \hbar ($= 1.0544 \times 10^{-27}$ erg sec) is Planck's constant divided by 2π . The position of an electron subjected to the influence of an atomic nucleus is very well defined (the force to which it is subjected is large). However, owing to Heisenberg's uncertainty principle, the electron momentum is ill defined. An electron has a continuous motion around the position it occupies. This motion exerts pressure on the surrounding medium, exactly as the thermal agitation of the particles of a gas exerts its pressure. This pressure is called the electron degeneracy pressure. This pressure, since it is nonthermal in origin, is, of course,

*profshukla@yahoo.de

independent of the electron temperature; the pressure of degenerate electrons increases with increasing electron number density. It is, however, only at very high densities that the degeneracy pressure becomes comparable to or larger than the thermal gas pressure. One then says that the plasma matter is in an exotic state, comprising degenerate electrons and positrons or holes.

Plasmas with degenerate electrons and positrons with number densities comparable with solids and temperatures of several electron volts fall under the category of dense matter (Ichimaru, 1982; Fortov, 2009) that appears in the core of giant planets (Horn, 1991; Chabrier *et al.*, 2006; Chabrier, 2009) and the crusts of old stars (Guillot, 1999). Dense compressed plasmas are currently of wide interest due to their applications to astrophysical and cosmological environments (Lai, 2001; Opher *et al.*, 2001; Benvenuto and De Vito, 2005; Harding and Lai, 2006), as well as to inertial fusion science involving intense laser-solid density plasma interaction experiments (Lindl, 1995; Hu and Keitel, 1999; Andreev, 2000; Mendonça, 2001; Son and Fisch, 2005; Marklund and Shukla, 2006; Salamin *et al.*, 2006; Glenzer *et al.*, 2007; Malkin *et al.*, 2007; Kritcher *et al.*, 2008; Glenzer and Redmer, 2009; Lee *et al.*, 2009; Neumayer *et al.*, 2010; Froula *et al.*, 2011) for inertial confinement fusion (Azechi *et al.*, 2006) based on the high-energy density plasma physics (Drake, 2009; 2010; Norreys *et al.*, 2009). Plasmlike collective behavior is well studied experimentally and theoretically in solid-state physics (Kittel, 1996), in which metals and semiconductors support both transverse optical modes and longitudinal electrostatic modes, such as plasmons and phonons on electron and ion time scales, and, in addition, various lattice modes. Plasmons and phonons are usually probed by measuring the energy of electrons which have been passed through thin foils, or by laser scattering techniques. For example, the dispersion relation of collective electron plasma waves has been measured for several metal specimen by using an electron velocity analyzer of Möllenstedt type (Watanabe, 1956). Collective dispersive behavior of plasmons, including shifts in the plasmon frequency due to quantum effects, in solid-density plasmas have been observed by Glenzer *et al.* (2007) and Neumayer *et al.* (2010) using spectrally resolved x-ray scattering techniques (Kritcher *et al.*, 2008; Lee *et al.*, 2009). In these experiments, powerful x-ray sources are employed for accessing narrow bandwidth spectral lines via collective Thomson scattering of light off electron-density fluctuations. These experimental techniques also allow accurate measurements of the electron velocity distribution function, temperature, and ionization state in the dense matter regime. Gregori and Gericke (2009) also proposed future experiments to measure low-frequency oscillations in plasmas when keV free-electron lasers will become available. Froula *et al.* (2011) summarized the measurement techniques using scattering of electromagnetic (EM) waves in plasmas, and recent experimental results from x-ray scattering experiments in dense plasmas reveal that quantum mechanical effects are indeed important (Glenzer *et al.*, 2007; Glenzer and Redmer, 2009).

Furthermore, due to recent experimental progress in femto-second pump-probe spectroscopy, the field of quantum plasmas is also gaining significant attention (Crouseilles *et al.*, 2008) in connection with the collective dynamics of an

ensemble of degenerate electrons in metallic nanostructures and thin metal films. The physics of quantum plasmas is also relevant in the context of quantum diodes (Ang *et al.*, 2003; Ang and Zhang, 2007; Shukla and Eliasson, 2008), nanophotonics and nanowires (Barnes *et al.*, 2003; Chang *et al.*, 2006; Shpatakovskaya, 2006), nanoplasmonics (Ozbay, 2006; Atwater, 2007; Maier, 2007; Marklund *et al.*, 2008; Stockman, 2011), high-gain quantum free-electron lasers (Serbeto *et al.*, 2008; 2009), microplasma systems (Becker *et al.*, 2006), and small semiconductor devices (Markowich *et al.*, 1990; Haug and Koch, 2004; Haug and Jauho, 2007; Manfredi and Hervieux, 2007), such as quantum wells and piezomagnetic quantum dots (Adolfath *et al.*, 2008). The latter can be used as nanoscale magnetic switches.

Collective interactions between an ensemble of degenerate electrons and positrons or holes give rise to novel waves and structures in quantum plasmas. Studies of linear waves in a nonrelativistic unmagnetized quantum plasma with degenerate electrons began with the pioneering theoretical works of Klimontovich and Silin (1952a, 1952b), Bohm (1953), Bohm and Pines (1953), Klimontovich and Silin (1961), and Pines (1961), who studied the dispersion properties of high-frequency electron plasma oscillations (EPOs). The frequencies of the latter with an arbitrary electron degeneracy have been found by Maafa (1993). In the theoretical description of the EPOs, Klimontovich and Silin and Bohm and Pines used the Wigner distribution function (Wigner, 1932) and the density matrix approach to demonstrate that in a quantum plasma with a Fermi-Dirac equilibrium distribution function for degenerate electrons, the frequency of the EPOs is significantly different from the Bohm-Gross frequency in a classical electron-ion plasma with nondegenerate electrons obeying the Maxwell-Boltzmann distribution function. The dispersion to the EPOs appears through the electron Fermi pressure and electron tunneling effects (Wilhelm, 1971; Gardner and Ringhofer, 1996; Manfredi and Haas, 2001; Manfredi, 2005; Jünger *et al.*, 2006; Shukla, 2006; Shukla and Eliasson, 2006; Misra, 2009; Shukla and Eliasson, 2010). The quantum Bohm potential, responsible for electron tunneling, appeared first in the quantum fluid description of a single electron by Madelung (1927) and Bohm (1953). For systems of degenerate electrons, different forms of the potential have been derived by using moments of the Wigner equation (Iafrate *et al.*, 1981; Ancona and Iafrate, 1989) and by using a variational approach (Feynman and Kleinert, 1986; Kleinert, 1986). They have been used in quantum hydrodynamic (QHD) equations (Wilhelm, 1971) for modeling nanodevices (Ferry and Zhou, 1993; Gardner and Ringhofer, 1996). More recently, Lagrangian approaches have been used to device efficient computational algorithms for quantum systems (Lopreore and Wyatt, 1999; Mayor *et al.*, 1999). These and other methods for computational QHD using quantum trajectories have been summarized by Wyatt (2005).

The quantum effects are important for the dielectric and dispersive properties of a quantum plasma. The longitudinal and transverse dielectric constants of an isotropic quantum plasma were worked out by Lindhard (1954), Silin and Rukhadze (1961), and Kuzeev and Rukhadze (1999). Contributions of the electron spin and exchange interactions to the EM wave dispersion relations in an unmagnetized

quantum plasma have been presented by Burt and Wahlquist (1962) by using a quantum kinetic theory. The quantum mechanical phase space distribution of Wigner (1932) has been further generalized by Brittin and Chappell (1962) for a system of charged particles including the quantized EM field and Green's functions involving correlations of distribution functions and vector potentials. Kinetic models for spin-polarized plasmas have been developed by Cowley *et al.* (1986), Zhang and Balescu (1988), and Balescu and Zhang (2009). More recently, electron spin-1/2 effects in a quantum magnetoplasma have also been considered by Brodin *et al.* (2008a) and Zamanian *et al.* (2010). The gauge problem in quantum kinetics has been treated by Stratonovich (1956) and Serimaa *et al.* (1986), which is important whenever the fields are not electrostatic. In a quantum magnetoplasma, one finds that the external magnetic field significantly affects the dynamics of degenerate electrons, and that the thermodynamics and kinetics (Steinberg, 2000) in a quantum magnetoplasma are significantly different from those in an unmagnetized quantum plasma. Oberman and Ron (1963) derived the expression for the dielectric function for longitudinal waves in a nonrelativistic magnetized quantum plasma and discussed applications of their work to heavily doped semiconductors. Kelly (1964) studied the dispersive properties of a magnetized quantum plasma by using the Wigner distribution function and the Maxwell equations. Finally, we mention that useful foundations for the theory of quantum plasmas are presented by de Groot and Suttorp (1972), while quantum kinetic models including the effects of spin are reviewed by Lee (1995).

During the last decade, there has been a surge in investigating new aspects of collective interactions in dense quantum plasmas by means of nonrelativistic quantum hydrodynamic (Gardner and Ringhofer, 1996; Manfredi and Haas, 2001; Manfredi, 2005; Jüngel *et al.*, 2006; Shukla and Eliasson, 2010) and quantum kinetic (Bonitz, 1998; Kremp *et al.*, 1999; Tsintsadze and Tsintsadze, 2009) equations. Models for non-ideal effects in a strongly coupled dense plasma have been presented by Carruthers and Zachariasen (1983), Kremp *et al.* (2005), and Redmer and Röpke (2010). The Wigner-Poisson model (Hillery *et al.*, 1984) has been used to derive a set of QHD equations (Manfredi and Haas, 2001; Manfredi, 2005) for electrostatic (ES) waves in a quantum plasma. The relation between the QHD and kinetic models have been investigated by Haas *et al.* (2010). The quantum nature (Manfredi and Haas, 2001; Shukla and Eliasson, 2010) is manifested in the nonrelativistic electron momentum equation through the quantum statistical pressure, which requires knowledge of the Wigner electron distribution function for a quantum mixture of electron wave functions, each characterized by an occupation probability. The quantum part of the electron pressure is also represented as a nonlinear quantum force (Wilhelm, 1971; Gardner and Ringhofer, 1996; Manfredi and Haas, 2001) $-\nabla\phi_B$, where $\phi_B = -(\hbar^2/2m_e\sqrt{n_e})\nabla^2\sqrt{n_e}$ is the Bohm potential, and m_e and n_e are the electron mass and electron number density, respectively. Defining the effective wave function $\psi = \sqrt{n_e(\mathbf{r}, t)}\exp[iS_e(\mathbf{r}, t)/\hbar]$, where $\nabla S_e(\mathbf{r}, t) = m_e\mathbf{u}_e(\mathbf{r}, t)$ and $\mathbf{u}_e(\mathbf{r}, t)$ is the electron fluid velocity, the nonrelativistic electron momentum equation can be cast into an effective nonlinear Schrödinger (NLS) equation (Manfredi and Haas, 2001; Manfredi, 2005; Shukla, 2006; Shukla and

Eliasson, 2006, 2010), in which there appears a coupling between the electron wave function and the ES potential associated with the EPOs. The ES potential, in turn, is determined from Poisson's equation. Thus, one has the coupled NLS and Poisson equations, governing the dynamics of nonlinearly interacting EPOs is a quantum plasma. Both non-relativistic QHD and NLS-Poisson equations exclude strong interactions among the quantum particles and electron-exchange interactions (Hohenberg and Kohn, 1964; Kohn and Sham, 1965) between an electron and the background plasma particles (e.g., degenerate electrons and nondegenerate ions). However, it has turned out that the QHD and NLS-Poisson equations have been quite useful for studying linear and nonlinear plasma waves, as well as stability of quantum plasmas (Manfredi and Haas, 2001; Haas *et al.*, 2003; Haas, 2005; Manfredi, 2005; Shukla, 2006; Shukla and Eliasson, 2006; Haas, 2007; Shukla and Eliasson, 2010) at nanoscales involving the quantum force (Wilhelm, 1971; Gardner and Ringhofer, 1996) and the quantum statistical pressure law for an unmagnetized quantum plasma with degenerate electrons. New effects also appear when one accounts for the potential energy of the electron spin 1/2 in a magnetic field (Takabayasi, 1955; Brodin and Marklund, 2007a, 2007b, 2007c; Marklund and Brodin, 2007; Misra, 2007, 2009; Shukla, 2007, 2009; Brodin *et al.*, 2008b, 2010; Misra and Samanta, 2010). In fact, the QHD model for degenerate electrons in both nonrelativistic (Manfredi and Haas, 2001; Manfredi, 2005; Shukla, 2006; Shukla and Eliasson, 2006, 2010) and relativistic (Masood *et al.*, 2010) quantum plasma regimes seems to provide an adequate description for probing some quantum collective interactions in compressed plasmas (Glenzer *et al.*, 2007; Glenzer and Redmer, 2009; Lee *et al.*, 2009; Neumayer *et al.*, 2010; Froula *et al.*, 2011) due to the availability of ultrafast x-ray Thompson scattering spectroscopic techniques.

In this Colloquium, we present the recent development of numerous nonlinear collective processes in a quantum plasma with degenerate electrons. We first describe the salient properties of quantum plasmas in which degenerate electrons follow the Fermi-Dirac distribution. We then present the relevant equations for describing linear and nonlinear wave phenomena in quantum plasmas. After reviewing the linear properties of ES and EM waves, we proceed by presenting numerical results of the governing nonlinear equations, which reveal localization of ES and EM waves at nanoscales. Specifically, we discuss the formation and dynamics of nanostructures (e.g., 1D quantum electron-density cavities and 2D quantum vortices), as well as discuss the properties of 3D quantum electron fluid turbulence at nanoscales. Also presented are nonlinear interactions between intense EM waves and ESOs, which reveal stimulated scattering of EM waves off quantum plasma oscillations and trapping of light into a quantum electron-density cavity. The effects of an external magnetic field on linear and nonlinear wave phenomena in a quantum magnetoplasma are examined. Finally, we highlight possible applications, as well as future perspectives and outlook of nonlinear quantum plasma physics.

II. BASIC PROPERTIES OF QUANTUM PLASMAS

We first summarize some of the basic properties of quantum plasmas that are quite distinct from classical plasmas.

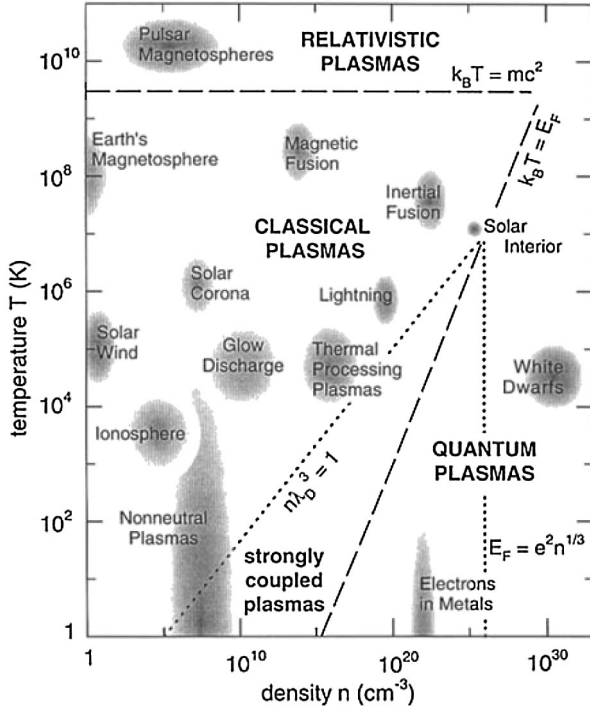


FIG. 1. The plasma diagram in the $\log T$ - $\log n_e$ plane, separating the classical and quantum regimes. From National Research Council 1995.

While classical plasmas are composed of nondegenerate plasma particles with low number densities and relatively high electron and ion temperatures, quantum plasmas have degenerate electrons and/or positrons with extremely high number densities and relatively low temperatures. The ions can usually be treated as nondegenerate plasma particles. Figure 1 shows the plasma parameter regimes (the electron temperature versus the electron number density) under which quantum plasmas occur in different physical environments.

Quantum mechanical effects start playing a significant role when the Wigner-Seitz radius (average interparticle distance) $a = (3/4\pi n)^{1/3}$ is comparable to or smaller than the thermal de Broglie wavelength $\lambda_B = \hbar/mv_T$, where m is the mass of the quantum particles (e.g., degenerate electrons, degenerate positrons, degenerate holes), $v_T = (k_B T/m)^{1/2}$ is the thermal speed of the quantum particles, T is the temperature, m is the mass, and k_B is the Boltzmann constant, i.e., when

$$n\lambda_B^3 \geq 1, \quad (1)$$

or, equivalently, when the temperature T is comparable to or lower than the Fermi temperature $T_F = E_F/k_B$, where the Fermi energy is

$$E_F = \frac{\hbar^2}{2m} (3\pi^2)^{2/3} n^{2/3}. \quad (2)$$

The relevant degeneracy parameter for the quantum plasma is

$$\frac{T_F}{T} = \frac{1}{2} (3\pi^2)^{2/3} (n\lambda_B^3)^{2/3} \geq 1. \quad (3)$$

For typical metallic densities of free electrons, $n \sim 5 \times 10^{22} \text{ cm}^{-3}$, we have $T_F \sim 6 \times 10^4 \text{ K}$, which should be compared with the usual temperature T .

When the plasma particle temperature approaches T_F , one can show, by using a density matrix formalism (Bransden and

Joachain, 2000), that the equilibrium distribution function changes from the Maxwell-Boltzmann $\propto \exp(-E/k_B T)$ to the Fermi-Dirac (FD) distribution function

$$\mathcal{F}_{\text{FD}} = 2 \left(\frac{m}{2\pi\hbar} \right)^3 \left[1 + \exp\left(\frac{E - \mu}{k_B T} \right) \right]^{-1}, \quad (4)$$

where in the nonrelativistic limit the energy is $E = (m/2)v^2 = (m/2)(v_x^2 + v_y^2 + v_z^2)$. The chemical potential is denoted by μ . The parameter $\mu/k_B T$ is large and negative in the nondegenerate limit, and is large and positive in the completely degenerate limit. The equilibrium electron number density associated with the FD distribution function is

$$n_0 = \int \mathcal{F}_{\text{FD}} d^3 v = -\frac{1}{4} \left(\frac{2mk_B T}{\pi\hbar^2} \right)^{3/2} \text{Li}_{3/2}[-\exp(\xi_\mu)], \quad (5)$$

where $\text{Li}_{3/2}$ is the polylogarithm function and $\xi_\mu = \mu/k_B T$. The completely degenerate limit corresponds to $\mu \rightarrow k_B T_F$ and $T_F \gg T$. The relation between T_F/T and ξ_μ is (Melrose 2008) $-\text{Li}_{3/2}[-\exp(\xi_\mu)] = (4/3\sqrt{\pi})(T_F/T)^{3/2}$.

It is useful to define the quantum coupling parameters for electron-electron and ion-ion interactions. The electron-electron Coulomb coupling parameter is defined as the ratio of the electrostatic interaction energy $E_{\text{int}} = e^2/a_e$ between electrons and the electron Fermi energy $E_{\text{Fe}} = k_B T_{\text{Fe}}$, where e is the magnitude of the electron charge and $a_e = (3/4\pi n_e)^{1/3}$ is the mean interelectron distance. We have

$$\Gamma_e = \frac{E_{\text{int}}}{E_{\text{Fe}}} \approx 0.3 \left(\frac{1}{n_e \lambda_{\text{Fe}}^3} \right)^{2/3} \approx 0.3 \left(\frac{\hbar \omega_{pe}}{k_B T_{\text{Fe}}} \right)^2, \quad (6)$$

where $\lambda_{\text{Fe}} = V_{\text{Fe}}/\omega_{pe}$, $V_{\text{Fe}} = (2E_{\text{Fe}}/m_e)^{1/2} = (\hbar/m_e)(3\pi^2 n_e)^{1/3}$ is the electron Fermi speed, and $\omega_{pe} = (4\pi n_e e^2/m_e)^{1/2}$ the electron plasma frequency. Furthermore, the ion-ion Coulomb coupling parameter is $\Gamma_i = Z_i^2 e^2/a_i k_B T_i$, where Z_i is the ion charge state, $a_i = (3/4\pi n_i)^{1/3}$ is the mean inter-ion distance, and T_i is the ion temperature.

Since Γ_e for metallic plasmas could be larger than unity, it is of interest to enquire the role of interparticle collisions on collective processes in a quantum plasma. It turns that the Pauli blocking reduces the collision rate for most practical purposes (Manfredi, 2005; Son and Fisch, 2005). Because of Pauli blocking, only electrons with a shell of thickness $k_B T$ about the Fermi surface suffer collisions. For these electrons, the electron-electron collision frequency is proportional to $k_B T/\hbar$. The average collision frequency among all electrons turns out to be (Manfredi, 2005)

$$v_{ee} = \frac{k_B T^2}{\hbar T_{\text{Fe}}}. \quad (7)$$

Typically, $v_{ee} \ll \omega_{pe}$ when $T < T_{\text{Fe}}$, which is relevant for metallic electrons. On the other hand, the typical time scale for electron-ion (lattice) collisions is $\tau_{ei} \approx 10 \text{ fs}$, which is 1 order of magnitude greater than the electron plasma period. Accordingly, a collisionless quantum plasma regime is relevant for phenomena appearing on the time scale of the order of a femtosecond in a metallic plasma.

In compact astrophysical objects such as white dwarf stars, the mean distance $n_e^{-1/3}$ between electrons become comparable to the Compton length $\lambda_C = \hbar/m_e c$, and accordingly the speed of an electron on the Fermi surface becomes comparable to

the speed of light c in vacuum, so that one has to take relativistic effects into account. Relativistic degenerate electrons are found in the core of massive white dwarf stars (Shapiro and Teukolsky, 1983; Koester and Chanmugam, 1990), aptly named due to their very low luminosities yet high surface emissivities, which are compact bodies with radii $\leq 10^{-2}R_\odot$ and masses typically $\leq M_\odot$. Consequently, the average electron number densities are quite high ($\sim 10^{30} \text{ cm}^{-3}$). Since electrons are fermions, only one electron can occupy a given quantum state (position, spin). In a simplified picture, each electron will on average occupy a volume $1/n_e$. Then, by Heisenberg's uncertainty principle (Bransden and Joachain, 2000) $\Delta x \Delta p \lesssim \hbar/2$, the mean momentum of electrons can be estimated to be $p_x \approx \hbar n_e^{1/3}$. If electrons are nonrelativistic, the velocity of the electron is $\sim p_x/m_e = \hbar n_e^{1/3}/m_e$; however, if electrons are relativistic, their velocity will be close to c . Now the electron pressure, as it is for a simple gas, is the momentum transfer per unit area, or $P_e = (\text{momentum}) \times (\text{velocity}) \times (\text{number density})$. For nonrelativistic electrons, we have (Gursky, 1976) $P_e = \hbar n_e^{1/3} (\hbar n_e^{1/3}/m_e) n_e = \hbar^2 n_e^{5/3}/m_e$. On the other hand, when electrons are relativistic, the relativistic electron pressure is $P_{er} = \hbar n_e^{1/3} c n_e = \hbar c n_e^{4/3}$. In the past, Chandrasekhar (1931a, 1931b, 1935, and 1939) and others presented a rigorous derivation of the electron pressure P_C for arbitrary relativistic electron degeneracy pressure in dense matter. It reads

$$P_C = \frac{\pi}{3\hbar^3} m_e^4 c^5 f(\xi_c), \quad (8)$$

where $f(\xi_c) = \xi_c (2\xi_c^2 - 3)(1 + \xi_c^2)^{1/2} + 3 \sinh^{-1}(\xi_c)$, $\xi_c = p_c/m_e c$, and $p_c = (3\hbar^3 n_e/8\pi)^{1/3}$ is the momentum of an electron on the Fermi surface. In the nonrelativistic limit $\xi_c \ll 1$, we have (Chandrasekhar, 1935, 1939)

$$P_n = \frac{\pi^{2/3}}{5m_e} \hbar^2 n_e^{5/3}, \quad (9)$$

while in the ultrarelativistic limit $\xi_c \gg 1$, the degenerate electron pressure reads (Chandrasekhar, 1931a)

$$P_u = \frac{(3\pi^2)^{1/3}}{4} \hbar c n_e^{4/3} \approx \frac{3}{4} \hbar c n_e^{4/3}. \quad (10)$$

Thus, the intuitively obtained formulas of Gursky (1976) for nonrelativistic and ultrarelativistic pressures for degenerate electrons are in agreement with those deduced from the pressure formula (8) for an arbitrary relativistic electron degeneracy pressure.

In his Nobel Prize winning papers on the structure of compact stars, Chandrasekhar (1931a and 1931b) balanced the gradient of the ultrarelativistic electron degeneracy pressure P_u/R and the gravitational force $G = (GM/R^2)n_e m_n$, where G is the gravitational constant, M and R are the mass and radius of a star, respectively, m_n is the mass of the nuclei ($n_e m_n = M/R^3$), to deduce the critical mass of a star $M_c = (\hbar c/G)^{3/2} m_n^{-2} \approx 1.4 M_\odot$, where M_\odot is the solar mass. The interior of white dwarf stars usually consists of fully ionized helium, carbon, and oxygen, which approximately consist of equal amounts of protons and neutrons. Hence, the effective mass of the nuclei can be taken to be the proton mass plus the neutron mass. Since M_c is independent of density, it means that this mass is obtained independent of radius. This is the limiting

mass; more massive stars cannot be supported by electron degeneracy pressure no matter how small they are. This was the discovery of Chandrasekhar; that the pressure dependence on density changed in going from nonrelativistic to relativistic conditions and, as a consequence, there arose a finite limit to the mass of a star with ultrarelativistic degenerate electrons.

III. MODEL EQUATIONS FOR QUANTUM PLASMAS

In quantum systems, the Dirac and Maxwell equations are often used to study the dynamics of a relativistic quantum particle or fermion (electrons and positrons) in the presence of intense electromagnetic fields. Quantum particles have spin. For example, an electron spin $s = 1/2$ is an intrinsic property of electrons, which have an intrinsic angular momentum characterized by quantum number $1/2$, and a magnetic moment for individual electrons. In fact, the relativistic Dirac equation provides a description of quantum particles (with spin) under the action of the electromagnetic fields. The spin of electrons (and positrons), which have the spin $1/2$, has been introduced through Dirac's Hamiltonian (Dirac, 1981)

$$\mathcal{H} = c \boldsymbol{\alpha}_s \cdot \left(\mathbf{p}_e + \frac{e}{c} \mathbf{A} \right) - e \phi + \boldsymbol{\beta} m_e c^2, \quad (11)$$

where $\mathbf{p}_e = -i\hbar \nabla$ is the momentum operator, and $\boldsymbol{\alpha}_s$ and $\boldsymbol{\beta}$ are the Dirac matrices. The three Cartesian components α_j ($j = 1, 2, 3$) of $\boldsymbol{\alpha}_s$ are usually constructed with help of the Pauli spin matrices σ_x , σ_y , and σ_z (Bransden and Joachain, 2000). The corresponding wave functions ψ are four-component spinors. The magnetic field is $\mathbf{B} = \nabla \times \mathbf{A}$, where \mathbf{A} and ϕ are the vector and scalar potentials, which are determined from the Maxwell equations.

In the nonrelativistic limit, the Pauli equation (Berestetskii *et al.*, 1999) in the presence of the electromagnetic fields describes the dynamics of a single quantum particle. It reads (Tsintsadze and Tsintsadze, 2009)

$$i\hbar \frac{\partial \psi_\alpha}{\partial t} = H_\alpha \psi_\alpha, \quad (12)$$

where

$$H_\alpha = -\frac{\hbar^2}{2m_\alpha} \nabla^2 - \frac{iq_\alpha \hbar}{2m_\alpha c} (\mathbf{A} \cdot \nabla + \nabla \cdot \mathbf{A}) + \frac{q_\alpha^2 \mathbf{A}^2}{2m_\alpha c^2} + q_\alpha \phi - \boldsymbol{\mu}_\alpha \cdot \mathbf{B} \quad (13)$$

is the Hamiltonian, and $\psi_\alpha(\mathbf{r}, t, \boldsymbol{\sigma})$ is the wave function of the single quantum particle species α with the spin $\mathbf{s} = (1/2)\boldsymbol{\sigma}$ ($|\boldsymbol{\sigma}| = 1$), and $q_\alpha = -e(+e)$ for electrons (positrons). The last term in Eq. (13) is the potential energy of the magnetic dipole in the external magnetic field, the magnetic moment of which is $\boldsymbol{\mu}_\alpha = (q_\alpha \hbar / 2m_\alpha c) \boldsymbol{\sigma} \equiv \boldsymbol{\mu}_B \boldsymbol{\sigma}$, where $\boldsymbol{\mu}_B = q_\alpha \hbar / 2m_e c$ is the Bohr-Pauli magneton and $\boldsymbol{\sigma}$ is the spin operator of a single quantum particle (Landau and Lifshitz, 1998a).

By using the Madelung representation (Madelung, 1927) for the complex wave function ψ_α , viz.

$$\psi_\alpha(\mathbf{r}, t, \boldsymbol{\sigma}) = \Psi_\alpha(\mathbf{r}, t, \boldsymbol{\sigma}) \exp(iS_\alpha/\hbar), \quad (14)$$

where $\Psi_\alpha(\mathbf{r}, t, \boldsymbol{\sigma})$ and $S_\alpha(\mathbf{r}, t, \boldsymbol{\sigma})$ are real, in the Pauli equation (12), we obtain the quantum Madelung fluid equations (Tsintsadze and Tsintsadze, 2009)

$$\frac{\partial n_\alpha}{\partial t} + \nabla \cdot (n_\alpha \mathbf{p}_\alpha / m_\alpha) = 0 \quad (15)$$

and

$$\frac{d\mathbf{p}_\alpha}{dt} = q_\alpha \left(\mathbf{E} + \frac{\mathbf{u}_\alpha \times \mathbf{B}}{c} \right) + \mathbf{F}_Q + \mathbf{F}_s, \quad (16)$$

where

$$\mathbf{F}_Q = \frac{\hbar^2}{2m_\alpha} \nabla \left(\frac{\nabla^2 \sqrt{n_\alpha}}{\sqrt{n_\alpha}} \right) \quad (17)$$

and

$$\mathbf{F}_s = \mu_B \nabla (\boldsymbol{\sigma} \cdot \mathbf{B}). \quad (18)$$

Here, $n_\alpha = |\Psi_\alpha|^2$ is the probability density of finding a single quantum particle with a spin \mathbf{s} at some point in space, $\mathbf{p}_\alpha = \nabla S_\alpha - q_\alpha \mathbf{A}/c$ is the momentum operator of a quantum particle, $d/dt = (\partial/\partial t) + \mathbf{u}_\alpha \cdot \nabla$, \mathbf{u}_α is the velocity of a quantum particle, and $\mathbf{E} = -\nabla\phi - c^{-1}\partial\mathbf{A}/\partial t$ and $\mathbf{B} = \nabla \times \mathbf{A}$.

The spin force \mathbf{F}_s in a quantum magnetoplasma can also be written as (Brodin and Marklund, 2007a; 2007b; 2007c; Brodin *et al.*, 2008b; Marklund and Brodin, 2007)

$$\mathbf{F}_s = \mu_B \tanh\left(\frac{\mu_B B}{k_B T_\alpha}\right) \nabla B, \quad (19)$$

where $B = |\mathbf{B}|$ and $\tanh(\xi) = B_{1/2}(\xi)$, with the Brillouin function with argument $1/2$ describing particles of spin $1/2$. The Langevin parameter $\tanh(\xi)$ accounts for the macroscopic magnetization of electrons due to the electron thermal agitation and electron-electron collisions.

A. The Schrödinger and Wigner-Poisson equations

The quantum N -body problem is governed by the Schrödinger equation for the N -particle wave function $\psi(q_1, q_2, \dots, q_N)$, where $q_j = (\mathbf{r}_j, s_j)$ is the coordinate (space, spin) of the particle j , each particle associated with energy \mathcal{E}_j . A drastic simplification occurs if one neglects the correlation between the particles at every order in Γ_Q and describes the full wave function as the product of the single-particle wave functions. For identical quantum particles, the N -particle wave function is given by the Slater determinant (Bransden and Joachain, 2000)

$$\psi(q_1, q_2, \dots, q_N) = \frac{1}{\sqrt{N!}} \begin{vmatrix} \psi_1(q_1, t) & \psi_2(q_1) & \dots & \psi_N(q_1) \\ \psi_1(q_2, t) & \psi_2(q_2) & \dots & \psi_N(q_2) \\ \vdots & \vdots & \ddots & \vdots \\ \psi_1(q_N) & \psi_2(q_N) & \dots & \psi_N(q_N) \end{vmatrix}, \quad (20)$$

which is *antisymmetric* with respect to an interchange of any two particle coordinates. This property is required by the Pauli exclusion principle under the second quantization procedure for a system of N identical nonrelativistic quantum particles. Accordingly, ψ vanishes if two rows are identical, i.e., two identical quantum particles cannot occupy the same state. As an example ($N = 2$): $\psi(q_1, q_2) = (1/\sqrt{2})[\psi_1(q_1)\psi_2(q_2) - \psi_1(q_2)\psi_2(q_1)]$ so that $\psi(q_2, q_1) = -\psi(q_1, q_2)$ and $\psi(q_1, q_1) = 0$. In the zero temperature limit,

all energy states up to the Fermi energy level are occupied, while no energy states above the Fermi level are occupied.

To capture collective effects in quantum plasmas, Haas *et al.* (2000) and Anderson *et al.* (2002) used the time-dependent Hartree model where electrons are described by a statistical mixture of N pure states, where each wave function ψ_j , $j = 1, \dots, N$, obeys the Schrödinger equation (Anderson *et al.*, 2002)

$$i\hbar \frac{\partial \psi_j}{\partial t} + \frac{\hbar^2}{2m_e} \nabla^2 \psi_j + e\phi \psi_j = 0, \quad (21)$$

which is coupled with Poisson's equation

$$\nabla^2 \phi = 4\pi e \left(\sum_{j=1}^N |\psi_j|^2 - Z_i n_i \right), \quad (22)$$

where n_i is the ion number density (to be obtained from the hydrodynamic equations for nondegenerate ions, to be discussed later), and ϕ is the electrostatic potential arising from the charge distribution of N electrons. Equations (21) and (22) have been used to study streaming instabilities (Anderson *et al.*, 2002) and other kinetic effects in a quantum system composed of an ensemble of electrons. Within the Hartree-Fock model, Eq. (21) can be further generalized by including the electron-exchange term resulting from the Pauli exclusion principle. The effect of exchange is for electrons of like spin to avoid each other. Each electron of a given spin is consequently surrounded by an "exchange hole," a small volume around the electron which like-spin electrons avoid. For the study of magnetic ordering in quantum dots doped with magnetic impurities, Eqs. (21) and (22) must also be enlarged by including a 3D quantum dots confining potential and a Vosko-Wilk-Nusair spin dependent exchange-correlation potential (Dharma-wardana and Perrot, 1995). Hence, the self-consistent model will go far beyond the Kohn-Sham description (Kohn and Sham, 1965) for treating the dynamics of correlated electrons in electron clusters, accounting for electron-exchange and electron-correlation effects. In the presence of time-dependent potentials, the properties and dynamics of many-electron systems can be investigated by using a time-dependent functional theory (Runge and Gross, 1984).

However, in a nonrelativistic quantum plasma with an ensemble of degenerate electrons, it is more appropriate to use the quantum statistical theory involving the Wigner distribution function (Wigner, 1932)

$$f_w(\mathbf{r}, \mathbf{v}) = \left(\frac{m_e}{2\pi\hbar} \right)^3 \int \exp(im_e \mathbf{v} \cdot \mathbf{R}/\hbar) \psi^*(\mathbf{r} + \mathbf{R}/2) \times \psi(\mathbf{r} - \mathbf{R}/2) d^3 R, \quad (23)$$

where the asterisk denotes the complex conjugate. Equation (23) has also been used by Moyal (1949) for studying the dynamics of electrons in a quantum system.

For electrostatic interactions in a quantum plasma, the Wigner-Poisson equations, to a leading order (in the limit of weak quantum coupling parameter Γ_e), can be written as

$$\frac{\partial f_w}{\partial t} + \mathbf{v} \cdot \nabla f_w = -\frac{iem_e^3}{(2\pi)^3 \hbar^4} \iint e^{im_e(\mathbf{v}-\mathbf{v}') \cdot \mathbf{R}/\hbar} \left[\phi \left(\mathbf{x} + \frac{\mathbf{R}}{2}, t \right) - \phi \left(\mathbf{x} - \frac{\mathbf{R}}{2}, t \right) \right] f_w(\mathbf{x}, \mathbf{v}', t) d^3 R d^3 v' \quad (24)$$

and

$$\nabla^2 \phi = 4\pi e \left(\int f_w d^3 v - Z_i n_i \right). \quad (25)$$

B. The QHD equations

The nonrelativistic QHD equations (Wilhelm, 1971) have been developed in condensed matter physics (Gardner and Ringhofer, 1996) and in plasma physics (Manfredi and Haas, 2001; Manfredi, 2005). The nonrelativistic QHD equations are composed of the electron continuity equation

$$\frac{\partial n_e}{\partial t} + \nabla \cdot (n_e \mathbf{u}_e) = 0, \quad (26)$$

the electron momentum equation (Wilhelm, 1971)

$$m_e \left(\frac{\partial \mathbf{u}_e}{\partial t} + \mathbf{u}_e \cdot \nabla \mathbf{u}_e \right) = e \nabla \phi - \frac{1}{n_e} \nabla P_e + \mathbf{F}_Q, \quad (27)$$

and Poisson's equation

$$\nabla^2 \phi = 4\pi e (n_e - Z_i n_i). \quad (28)$$

In a quantum plasma with nonrelativistic degenerate electrons, the quantum statistical pressure in the zero electron temperature limit can be modeled as (Manfredi and Haas 2001; Crouseilles *et al.* 2008)

$$P_e = \frac{m_e V_{Fe}^2 n_0}{3} \left(\frac{n_e}{n_0} \right)^{(D+2)/D}, \quad (29)$$

where D is the number of space dimension of the system and $V_{Fe} = (\hbar/m_e)(3\pi^2 n_e)^{1/3}$ is the electron Fermi speed.

C. The NLS-Poisson equations

For investigating nonlinear properties of dense quantum plasmas, it is appropriate to work with a NLS equation. Hence, by introducing the wave function

$$\psi(\mathbf{r}, t) = \sqrt{n_e(\mathbf{r}, t)} \exp\left(i \frac{S_e(\mathbf{r}, t)}{\hbar}\right), \quad (30)$$

where S_e is defined according to $m_e \mathbf{u}_e = \nabla S_e$ and $n_e = |\psi|^2$, it can be shown that Eq. (27) can be cast into a NLS equation (Manfredi and Haas, 2001; Manfredi, 2005)

$$i\hbar \frac{\partial \psi}{\partial t} + \frac{\hbar^2}{2m_e} \nabla^2 \psi + e\phi \psi - \frac{m_e V_{Fe}^2}{2n_0^2} |\psi|^{4/D} \psi = 0, \quad (31)$$

where the electrostatic field ϕ is determined from Poisson's equation

$$\nabla^2 \phi = 4\pi e (|\psi|^2 - Z_i n_i). \quad (32)$$

We note that the third and fourth terms on the left-hand side of Eq. (31) represent the nonlinearities associated with the nonlinear coupling between the electrostatic potential and the electron wave function and the nonlinear quantum statistical pressure, respectively.

IV. LINEAR WAVES IN QUANTUM PLASMAS

A. Electron plasma oscillations

Linearization of the NLS-Poisson equations (31) and (32) around the equilibrium state and combining the resultant equations, we obtain the frequency ω of the EPOs (Klimontovich and Silin, 1952a; 1952b; Bohm, 1953; Bohm and Pines, 1953)

$$\omega = \left(\omega_{pe}^2 + \frac{3}{5} k^2 V_{Fe}^2 + \frac{\hbar^2 k^4}{4m_e^2} \right)^{1/2}, \quad (33)$$

where k is the wave number and $\omega_{pe} = (4\pi n_0 e^2 / m_e)^{1/2}$ is the electron plasma frequency. Here the ions are assumed to be stationary.

One can identify two distinct dispersion effects from Eq. (33): One long wavelength regime with $V_{Fe} \gg \hbar k / 2m_e$, and the other short wavelength regime with $V_{Fe} \leq \hbar k / 2m_e$. These two regimes are separated by the critical wave number

$$k_{\text{crit}} = \frac{2\pi}{\lambda_{\text{crit}}} \approx \frac{\pi \hbar}{m_e V_{Fe}} \sim n_e^{-1/3}. \quad (34)$$

It should be mentioned here that the quantum dispersion effects associated with the EPOs have recently been observed in a compressed plasma (Glenzer *et al.*, 2007; Neumayer *et al.*, 2010; Froula *et al.*, 2011). In compressed plasma experiments, powerful x-ray sources are employed for accessing narrow bandwidth electron plasma wave spectral lines via collective Thomson scattering in which powerful light scatters off electron-density fluctuations. We note that the dispersion relation for EPOs in the finite electron temperature limit is given by (Thiele *et al.*, 2008)

$$\omega^2 = \omega_{pe}^2 + 3k^2 V_{Te}^2 (1 + 0.088 n_e \Lambda_e^3) + \frac{\hbar^2 k^4}{4m_e^2}, \quad (35)$$

where $V_{Te} = (k_B T_e / m_e)^{1/2}$ is the electron thermal speed and $\Lambda_e = \sqrt{2\pi \hbar} / \sqrt{m_e k_B T_e}$ is the thermal (de Broglie) wavelength.

As mentioned in the Introduction, in the past many derived the dielectric constant for the high-frequency (in comparison with the ion plasma frequency) ES waves (Klimontovich and Silin, 1952a; 1952b; Bohm, 1953; Bohm and Pines, 1953; Lifshitz and Pitaevskii, 1981) and the refractive index for EM waves (Burt and Wahlquist, 1962) by using a quantum kinetic theory based on the Wigner and Poisson-Maxwell equations in a quantum plasma. In the following, we briefly discuss the well-known results for the ES (Klimontovich and Silin, 1952a; 1952b; Bohm, 1953; Bohm and Pines, 1953) and EM (Burt and Wahlquist, 1962) waves in an unmagnetized quantum plasma.

The dielectric constant for ES waves in a plasma with completely degenerate electrons reads (Lifshitz and Pitaevskii, 1981)

$$D_e(\omega, \mathbf{k}) = 1 + \frac{3\omega_{pe}^2}{2k^2 V_{Fe}^2} [1 - g(\omega_+) + g(\omega_-)], \quad (36)$$

where $\omega_{\pm} = \omega \pm \hbar k^2 / 2m_e$, and

$$g(\omega_{\pm}) = \frac{m_e (\omega_{\pm}^2 - k^2 V_{Fe}^2)}{2\hbar k V_{Fe}} \log \left(\frac{\omega_{\pm} + k V_{Fe}}{\omega_{\pm} - k V_{Fe}} \right). \quad (37)$$

Assuming that the phase velocity (ω/k) of the ES wave is much larger than V_{Fe} , we obtain by setting $D_e(\omega, \mathbf{k}) = 0$ the frequency of the EPOs, given by (36). On the other hand, in the semiclassical limit, viz. $\hbar |\mathbf{k}| \ll p_{Fe} = \hbar (3\pi^2 n_e)^{1/3}$, we have (Lifshitz and Pitaevskii, 1981) from Eq. (36)

$$D_e(\omega, \mathbf{k}) = 1 + \frac{3\omega_{pe}^2}{k^2 V_{Fe}^2} \left(1 - \frac{\omega}{2k V_{Fe}} \log \left| \frac{\omega + k V_{Fe}}{\omega - k V_{Fe}} \right| \right), \quad (38)$$

which in the short wavelength limit, viz. $k V_{Fe} \gg \omega_{pe}$, yields the so-called electron thermal quasimode (Klimontovich and Silin, 1952a; 1952b; 1961)

$$\omega = kV_{\text{Fe}}[1 + 2\exp(-2k^2\lambda_s^2 - 2)], \quad (39)$$

where $\lambda_s = \lambda_{\text{Fe}}/\sqrt{3}$ is the Thomas-Fermi screening length.

Furthermore, when $\omega = 0$, Eq. (38) as a function of k has a Kohn singularity at $\hbar k = 2p_{\text{Fe}}$, which is the diameter of the Fermi sphere. Here we have

$$D_e(0, \mathbf{k}) = 1 + \frac{e^2}{2\pi\hbar E_F} [1 - \xi \log(1/|\xi|)], \quad (40)$$

where $\xi = (\hbar k - 2p_{\text{Fe}})/2p_{\text{Fe}}$ and $|\xi| \ll 1$. In a quantum plasma, with $D(0, \mathbf{k})$ given by Eq. (38), the potential distribution $\varphi(r)$ around a stationary test charge q_t is

$$\varphi(r) = \frac{4\pi q_t}{(2\pi)^3} \int \frac{\exp(i\mathbf{k} \cdot \mathbf{r}) d^3k}{k^2 D_e(0, \mathbf{k})}, \quad (41)$$

which gives (Else *et al.*, 2010)

$$\varphi(r) \approx q_t \frac{12\lambda_{\text{Fe}}^2 \eta^4}{(2 + 3\eta^2)^2} \frac{\cos(2k_F r)}{r^3}, \quad (42)$$

where $\eta = \hbar\omega_{pe}/4k_B T_{\text{Fe}}$ and $k_F = p_{\text{Fe}}/\hbar$. We note that Eq. (42), which is proportional to $r^{-3} \cos(2k_F r)$, considerably differs from the Debye-Hückel shielding potential that is proportional to $r^{-1} \exp(-r/\lambda_{\text{De}})$ in a classical plasma with the Maxwell-Boltzmann electron distribution function. Here λ_{De} is the electron Debye radius. We further note that the shielding of a moving test charge in an unmagnetized quantum plasma has been investigated by Else *et al.* (2010) both analytically and numerically.

B. Ion plasma oscillations (IPOs)

We now focus our attention on the effect of the dynamics of nonrelativistic and nondegenerate ions in an unmagnetized quantum plasma. The dynamics of strongly coupled ions is governed by the ion hydrodynamic equations composed of Poisson's equation (28), and the continuity and momentum equations. The latter are

$$\frac{\partial n_i}{\partial t} + \nabla \cdot (n_i \mathbf{u}_i) = 0 \quad (43)$$

and

$$\left(1 + \tau_m \frac{\partial}{\partial t}\right) \left[\left(\frac{\partial}{\partial t} + \mathbf{u}_i \cdot \nabla \right) \mathbf{u}_i + \frac{Z_i e}{m_i} \nabla \phi + \frac{\gamma_i k_B T_i}{m_i n_i} \nabla n_i \right] - \frac{\eta}{\rho_i} \nabla^2 \mathbf{u}_i - \frac{(\xi + \frac{\eta}{3})}{\rho_i} \nabla (\nabla \cdot \mathbf{u}_i) = 0, \quad (44)$$

where n_i is the ion number density, \mathbf{u}_i is the ion fluid velocity, m_i is the ion mass, $\rho_i = n_i m_i$ is the ion mass density, γ_i is the adiabatic index for the ion fluid, τ_m is the viscoelastic relaxation time for ions, η and ξ are the bulk ion viscosities. The viscoelastic equation (44) for strongly systems has been successfully used (Ichimaru and Tanaka, 1986; Kaw and Sen, 1998) for investigating collective processes in classical plasmas with nondegenerate plasma particles.

The ions are coupled with degenerate electrons by the space charge electric field $\mathbf{E} = -\nabla\phi$. For low-phase velocity (in comparison with the electron Fermi speed) ES waves, we can neglect the inertia of the electrons to obtain

$$n_e \nabla \phi - \frac{9}{5} \frac{\hbar^2}{m_e} \nabla n_e^{5/3} + \frac{\hbar^2 n_e}{2m_e} \nabla \left(\frac{\nabla^2 n_e}{\sqrt{n_e}} \right) = 0, \quad (45)$$

for a quantum plasma with weakly relativistic degenerate electrons, while for a quantum plasma with ultrarelativistic degenerate electrons, we have

$$n_e \nabla \phi - 3/4 \hbar c \nabla n_e^{4/3} = 0. \quad (46)$$

Because of the ion inertia, one has new dielectric constants for the low-frequency (in comparison with the electron plasma frequency) ES waves (Pines, 1983; Pines and Nozieres, 1989; Eliasson and Shukla, 2008a; Shukla and Eliasson, 2008; Mushtaq and Melrose, 2009). In a quantum plasma with nonrelativistic degenerate electrons with $\omega^2 \ll k^2 V_{\text{Fe}}^2 + \hbar^2 k^4 / 4m_e^2$, we can linearize Eqs. (28) and (43)–(45), Fourier transform them, and combine the resultant equations to obtain

$$D_i(\omega, \mathbf{k}) = 1 + \frac{3\omega_{pe}^2}{k^2 V_{\text{Fe}}^2 + \hbar^2 k^4 / 4m_e^2} - \frac{\omega_{pi}^2}{\Omega_i^2}, \quad (47)$$

where $\omega_{pi} = (4\pi n_0 Z_i^2 e^2 / m_i)^{1/2}$ is the ion plasma frequency, and $\Omega_i^2 = \omega^2 - \gamma_i k^2 V_{\text{Ti}}^2 + i\omega k^2 \eta_*/(1 - i\omega\tau_m)$, with $V_{\text{Ti}} = (k_B T_i / m_i)^{1/2}$ and $\eta_* = (\xi + 4\eta/3) / m_i n_0$. On the other hand, in a quantum plasma with ultrarelativistic degenerate electrons, we have from Eqs. (28), (43), (44), and (46)

$$D_i(\omega, \mathbf{k}) = 1 + \frac{\omega_{pe}^2}{k^2 C_h^2} - \frac{\omega_{pi}^2}{\Omega^2}, \quad (48)$$

where $C_h^2 = c^2 \lambda_C n_0^{1/3}$, and $\lambda_C = \hbar / m_e c$ is the Compton length. By setting $D_i(\omega, \mathbf{k}) = 0$, we obtain the frequencies of the IPOs. For the case with nonrelativistic degenerate electrons, we have

$$\omega^2 = \gamma_i k^2 V_{\text{Ti}}^2 + \frac{k^2 \eta_*}{\tau_m} + \frac{\omega_{pi}^2 k^2 \lambda_{Th}^2}{1 + k^2 \lambda_{Th}^2}, \quad (49)$$

while for the case with ultrarelativistic degenerate electrons the result is

$$\omega^2 = \gamma_i k^2 V_{\text{Ti}}^2 + \frac{k^2 \eta_*}{\tau_m} + \frac{\omega_{pi}^2 k^2 \lambda_h^2}{1 + k^2 \lambda_h^2}, \quad (50)$$

where we have assumed $\omega\tau_m \ll 1$ and denoted $\lambda_{Th} = (\lambda_s^2 + \hbar^2 k^2 / 4m_e^2 \omega_{pe}^2)^{1/2}$, and $\lambda_h = C_h / \omega_{pe}$. The domain of validity of the hydrodynamic description for the ions in the context of ion oscillations in a weakly relativistic dense plasma has also been recently discussed (Mithen *et al.*, 2011).

Melrose and Mushtaq (2009) and Mushtaq and Melrose (2009) presented Landau damping rates for both electron and ion plasma waves in an unmagnetized dense quantum plasma. The imaginary parts of the dielectric constants can be used to calculate the structural form factor (Ichimaru, 1982) in quantum a plasma with degenerate electrons.

Shukla and Eliasson (2008) used the dielectric constant (47) without the quantum statistical pressure term (viz. the V_{Fe}^2 term) to investigate the screening and wake potentials around a test charge in an electron-ion quantum plasma. They found a new screening potential

$$\phi_{se} = \frac{q_t}{r} \exp(-k_q r) \cos(k_q r), \quad (51)$$

and the wake potential

$$\phi_w = - \frac{q_t}{|z - u_0 t|} \cos \left[\frac{\omega_{pi}}{u_0} (z - u_0 t) \right], \quad (52)$$

where $k_q = \sqrt{2}/\sqrt{\hbar/m_e\omega_{pe}}$ is the quantum wave number, and $r = [x^2 + y^2 + (z - u_0 t)^2]^{1/2}$ is the distance from the test charge moving with the speed u_0 along the z axis in a Cartesian coordinate system. The wake potential (52) behind a test charge arises due to collective interactions between a test charge and the ion oscillation with the frequency $\omega_k \approx \omega_{pi} k_{\perp} / (k_{\perp}^2 + k_q^2)^{1/2}$, with $k_z \ll k_q$, $k_{\perp} = (k_x^2 + k_y^2)^{1/2}$. We note that the Shukla-Eliasson exponential cosine-screened Coulomb potential ϕ_{se} has a minimum of $\phi_{se} \approx -0.02q_1 k_q$ at $r \approx 3k_q^{-1}$, similar to the Lennard-Jones potential for atoms. The Shukla-Eliasson screening potential ϕ_{se} , which is independent of the test charge speed u_0 , is different from the Yukawa screening potential $(q_t/r) \exp(-r/\lambda_s)$ that is valid in the limit $V_{Fe} \gg \hbar k/2m_e$. Recently, several (Ghoshal and Ho, 2009a; 2009b; Xia *et al.*, 2010) used the Shukla-Eliasson potential to study doubly excited resonance states of helium and hydrogen atoms embedded in a quantum plasma (Ghoshal and Ho, 2009a; 2009b), and lattice waves in 2D hexagonal quantum plasma crystals (Xia *et al.*, 2010).

Furthermore, by using D_i from Eq. (48), one can deduce potential distributions around a moving test charge in a quantum plasma with ultrarelativistic electrons. We have

$$\phi(r, z) = \frac{q_t}{r} \exp\left(-\frac{r}{\Lambda_C}\right) + \frac{q_t}{|z - u_0 t|} \cos\left(\frac{z - u_0 t}{L_c}\right), \quad (53)$$

where $\Lambda_C = C_{\hbar}/\omega_{pe}$ and $L_c = \lambda_c(M^2 - 1)^{1/2} > 0$, with $M = u_0/C_{\hbar}$.

C. High-frequency EM waves

Finally, we turn our attention to the high-frequency (HF) EM waves in an unmagnetized quantum plasma. Noting that HF-EM waves in the latter do not give rise to any density perturbations, we have the EM wave frequency

$$\omega = (k^2 c^2 + \omega_{pe}^2)^{1/2}. \quad (54)$$

However, consideration of the electron spin current and electron-exchange potential contributions in a quantum plasma gives rise to additional contributions to the refractive index N . We have (Burt and Wahlquist, 1962)

$$\frac{k^2 c^2}{\omega^2} = N \approx 1 - \frac{\omega_{pe}^2}{\omega^2} - \frac{\omega_{pe}^2 \hbar^2 k^2}{m_e^2 \omega^4} \left(\frac{1}{5} K_F^2 + \frac{1}{4} k^2 \right), \quad (55)$$

which includes the electron spin correction, and is valid at zero temperature. Here $\hbar K_F = (2m_e E_{Fe})^{1/2}$ is the momentum of degenerate electrons at the Fermi surface, the $(1/5)K_F^2$ term is related to the leading quantum term from the ordinary transverse current, and the $k^2/4$ term arises from the electron spin interactions. On the other hand, the EM wave dispersion relation, which accounts for the electron-exchange potential and discards the spin correction, reads (Burt and Wahlquist, 1962)

$$\frac{k^2 c^2}{\omega^2} = N \approx 1 - \frac{\omega_{pe}^2}{\omega^2} - \frac{\omega_{pe}^2 \hbar^2 k^2 K_F^2}{5m_e^2 \omega^4} + \frac{3\omega_{pe}^2 k^2}{40\omega^4 K_F^2}. \quad (56)$$

V. QUANTUM DARK SOLITONS AND VORTICES

We now discuss nonlinear properties and dynamics of 1D quantum dark solitons (characterized by the local electron-

density depletion associated with a positive potential) and 2D azimuthally symmetric electron vortices in an unmagnetized quantum plasma (Shukla and Eliasson, 2006) with immobile ions. The assumption of stationary ions is justified because we are looking for the nonlinear phenomena on a time scale much shorter than the ion plasma period.

We use the normalized NLS-Poisson equations (Shukla, 2006; Shukla and Eliasson, 2006)

$$i \frac{\partial \Psi}{\partial t} + \mathcal{A} \nabla^2 \Psi + \varphi \Psi - |\Psi|^{4/D} \Psi = 0 \quad (57)$$

and

$$\nabla^2 \varphi = |\Psi|^2 - 1, \quad (58)$$

where the time and space variables are in units of $\hbar/k_B T_{Fe}$ and the electron Fermi-Thomas screening length λ_{TF} , respectively. Furthermore, we have denoted $\Psi = \psi/\sqrt{n_0}$, $\varphi = e\phi/k_B T_{Fe}$, and $\mathcal{A} = 2\pi n_0^{1/3} e^2/k_B T_{Fe}$. The system (57) and (58) is supplemented by

$$\frac{\partial \mathbf{E}_{\varphi}}{\partial t} = i \mathcal{A} (\Psi \nabla \Psi^* - \Psi^* \nabla \Psi), \quad (59)$$

where $\mathbf{E}_{\varphi} = -\nabla \varphi$. Equations (57)–(59) have the following conserved integrals (Shukla and Eliasson, 2006; Shaikh and Shukla, 2007): the number of electrons

$$N = \int |\Psi|^2 d^3x, \quad (60)$$

the electron momentum

$$\mathbf{P} = -i \int \Psi^* \nabla \Psi d^3x, \quad (61)$$

the electron angular momentum

$$\mathbf{L} = -i \int \Psi^* \mathbf{r} \times \nabla \Psi d^3x, \quad (62)$$

and the total energy

$$\mathcal{E} = \iint \left[-\mathcal{A} \Psi^* \nabla^2 \Psi + \frac{|\nabla \varphi|^2}{2} + \frac{D}{(2+D)} |\Psi|^{(2+4/D)} \right] d^3x. \quad (63)$$

A. Quantum electron cavity

For quasistationary, 1D nonlinear structures moving with a constant speed v_0 , one can find solitary wave solutions of Eqs. (57) and (58) by introducing the ansatz $\Psi = W(\xi) \times \exp(iK_s x - i\Omega_s t)$, where W is a complex-valued function of the argument $\xi = x - v_0 t$, and K_s and Ω_s are a constant wave number and frequency shift, respectively. By the choice $K_s = v_0/2\mathcal{A}$, the coupled system of equations (57) and (58) can then be written as

$$\frac{d^2 W}{d\xi^2} + \lambda W + \frac{\varphi W}{\mathcal{A}} - \frac{|W|^4 W}{\mathcal{A}} = 0 \quad (64)$$

and

$$\frac{d^2 \varphi}{d\xi^2} = |\Psi|^2 - 1, \quad (65)$$

where $\lambda = (\Omega_s/\mathcal{A}) - v_0^2/4\mathcal{A}^2$ is an eigenvalue of the system. From the boundary conditions $|W| = 1$ and $\varphi = 0$ at $|\xi| = \infty$, we determine $\lambda = 1/\mathcal{A}$ and $\Omega_s = 1 + v_0^2/4\mathcal{A}$.

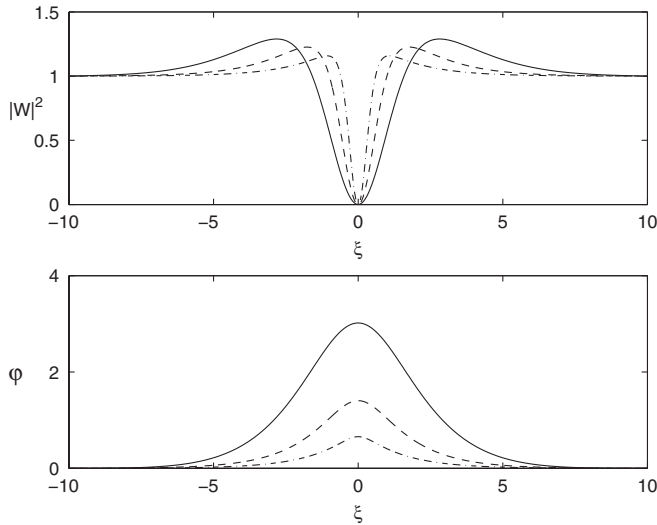


FIG. 2. The electron density $|W|^2$ (upper panel) and ES potential φ (lower panel) associated with a dark soliton supported by the system of Eqs. (64) and (65), for $\mathcal{A} = 5$ (solid lines), $\mathcal{A} = 1$ (dashed lines), and $\mathcal{A} = 0.2$ (dash-dotted line). From Shukla and Eliasson 2006.

The system of Eqs. (64) and (65) admits a first integral in the form

$$H_h = \mathcal{A} \left| \frac{dW}{d\xi} \right|^2 - \frac{1}{2} \left(\frac{d\varphi}{d\xi} \right)^2 + |W|^2 - \frac{|W|^6}{3} + \varphi |W|^2 - \varphi - \frac{2}{3} = 0, \quad (66)$$

where the boundary conditions $|W| = 1$ and $\varphi = 0$ at $|\xi| = \infty$ have been employed.

Figure 2 shows profiles of $|W|^2$ and φ obtained numerically from Eqs. (64) and (65) for a few values of \mathcal{A} , where W was set to -1 on the left boundary and to $+1$ on the right boundary, i.e., the phase shift is 180° between the two boundaries. The solutions are in the form of dark solitons, with a localized depletion of the electron density $N_e = |W|^2$, associated with a localized positive potential. Larger values of the quantum coupling parameter \mathcal{A} give rise to larger amplitude and wider dark solitons. The solitons localized “shoulders” on both sides of the density depletion.

A numerical solution of the time-dependent system of Eqs. (57) and (58) is shown in Fig. 3, with initial conditions close (but not equal) to the ones in Fig. 2. Two very clear and long-lived dark solitons are visible, associated with a positive potential of $\varphi \approx 3$, in agreement with the quasistationary solution of Fig. 2 for $\mathcal{A} = 5$. In addition, there are oscillations and wave turbulence in the time-dependent solution shown in Fig. 3. Hence, the dark solitons seem to be robust structures that can withstand perturbations and turbulence during a considerable time.

B. Quantum electron vortices

For two-dimensional ($D = 2$) EPOs in quantum plasmas, one can look for quantum vortex structures of the form

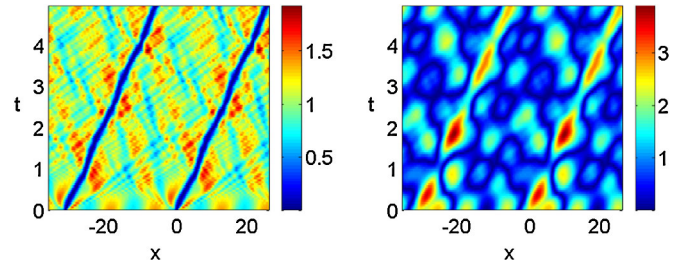


FIG. 3 (color online). The time development of the electron density $|\Psi|^2$ (left-hand panel) and ES potential φ (right-hand panel), obtained from a simulation of the system of Eqs. (57) and (58). The initial condition is $\Psi = 0.18 + \tanh[20 \sin(x/10)] \times \exp(iK_s x)$, with $K_s = v_0/2\mathcal{A}$, $\mathcal{A} = 5$, and $v_0 = 5$. From Shukla and Eliasson 2006.

$\Psi = \psi(r) \exp(is\theta - i\Omega_v t)$, where r and θ are the polar coordinates defined via $x = r \cos(\theta)$ and $y = r \sin(\theta)$, Ω_v is a constant frequency shift, and $s = 0, \pm 1, \pm 2, \dots$ for different excited states (charge states). With this ansatz, Eqs. (57) and (58) can be written as

$$\left[\Omega_v + \mathcal{A} \left(\frac{d^2}{dr^2} + \frac{1}{r} \frac{d}{dr} - \frac{s^2}{r^2} \right) + \varphi - |\psi|^2 \right] \psi = 0 \quad (67)$$

and

$$\left(\frac{d^2}{dr^2} + \frac{1}{r} \frac{d}{dr} \right) \varphi = |\psi|^2 - 1, \quad (68)$$

respectively, where the boundary conditions $\psi = 1$ and $\varphi = d\psi/dr = 0$ at $r = \infty$ determine the constant frequency $\Omega_v = 1$. Different signs of the charge state s describe different rotation directions of the quantum vortex. For $s \neq 0$, one must have $\psi = 0$ at $r = 0$, and from symmetry considerations one has $d\varphi/dr = 0$ at $r = 0$. Figure 4 shows numerical solutions of Eqs. (67) and (68) for different values of s and for $\mathcal{A} = 5$. Here a quantum vortex is characterized by a complete

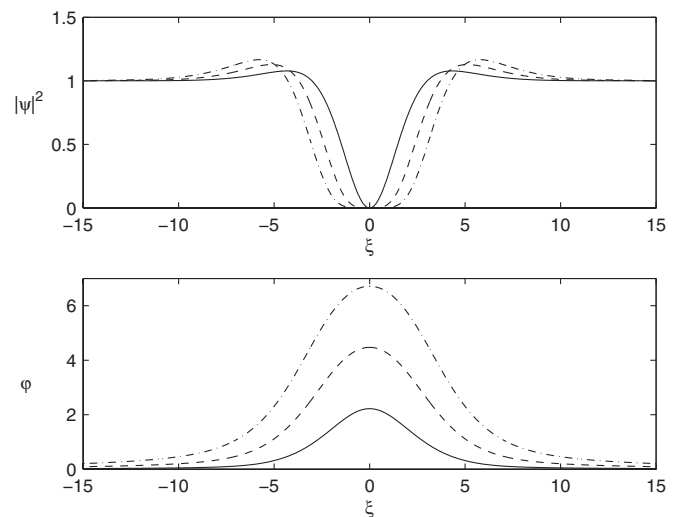


FIG. 4. The electron density $|\Psi|^2$ (upper panel) and ES potential φ (lower panel) associated with 2D electron vortices supported by the system (67) and (68), for the charge states $s = 1$ (solid lines), $s = 2$ (dashed lines), and $s = 3$ (dash-dotted lines), with $\mathcal{A} = 5$ in all cases. From Shukla and Eliasson 2006.

depletion of the electron density at the core of the vortex, and is associated with a positive ES potential.

A time-dependent solution of Eqs. (57) and (58) in two-space dimensions for singly charged ($s = \pm 1$) electron vortices is shown in Fig. 5, where, in the initial condition, four vortexlike structures were placed at some distance from each other. The initial conditions were such that the vortices are organized in two vortex pairs, with $s_1 = +1$, $s_2 = -1$, $s_3 = -1$, and $s_4 = +1$, seen in the upper panels of Fig. 5. The vortices in the pairs have opposite polarity on the electron fluid rotation, as seen in the upper right panel of Fig. 5. Interestingly, the “partners” in the vortex pairs attract each other and propagate together with a constant velocity, and in the collision and interaction of the vortex pairs (see the second and third pairs of panels in Fig. 5), the vortices keep their identities and change partners, resulting into two new vortex pairs which propagate obliquely to the original propagation direction. On the other hand, as shown in Fig. 6, vortices that are multiply charged ($|s_j| > 1$) are unstable. Here the system of Eqs. (57)

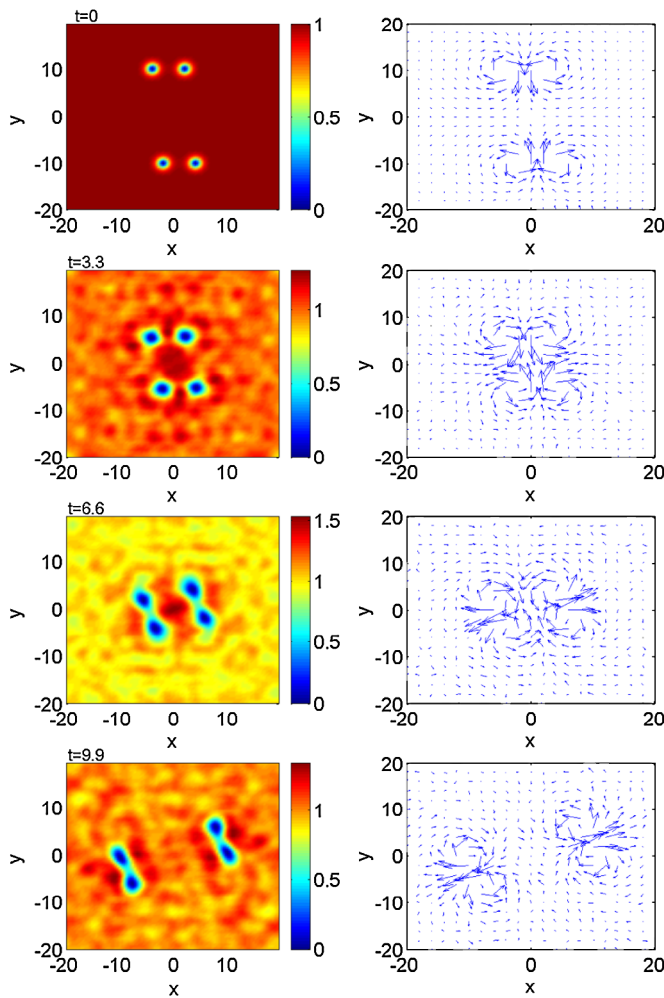


FIG. 5 (color online). The electron density $|\Psi|^2$ (left panel) and an arrow plot of the electron current $i(\Psi\nabla\Psi^* - \Psi^*\nabla\Psi)$ (right panel) associated with singly charged ($|s| = 1$) 2D electron vortices, obtained from a simulation of the time-dependent system of Eqs. (57) and (58), at times $t = 0$, $t = 3.3$, $t = 6.6$, and $t = 9.9$ (upper to lower panels), with $\mathcal{A} = 5$. The singly charged vortices form pairs and keep their identities. From Shukla and Eliasson 2006.

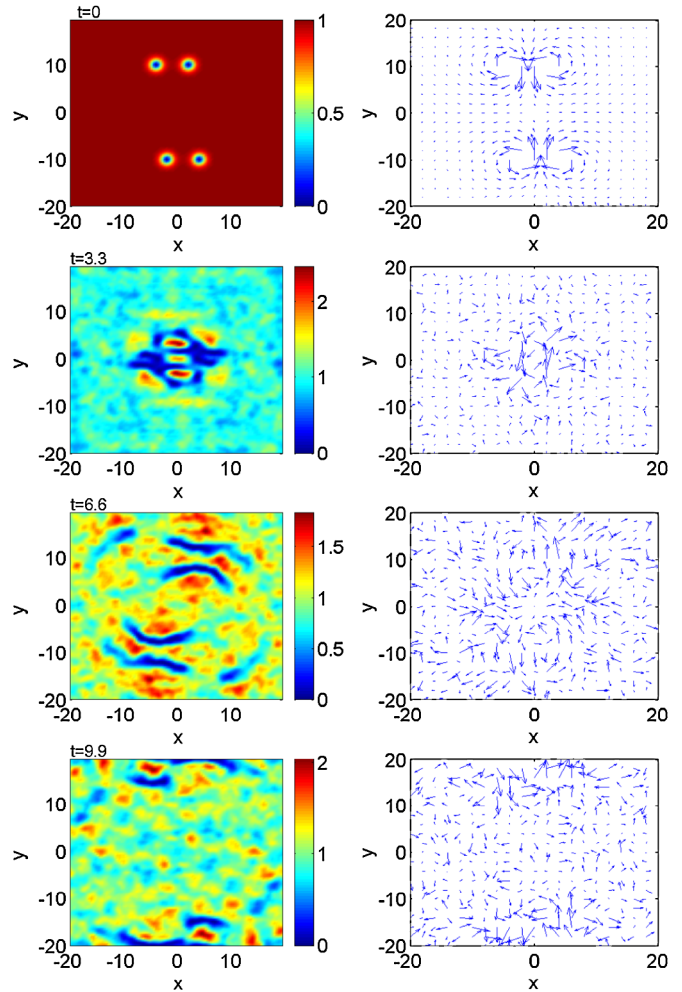


FIG. 6 (color online). The electron density $|\Psi|^2$ (left panel) and an arrow plot of the electron current $i(\Psi\nabla\Psi^* - \Psi^*\nabla\Psi)$ (right panel) associated with double charged ($|s| = 2$) 2D electron vortices, obtained from a simulation of the time-dependent system of Eqs. (57) and (58), at times $t = 0$, $t = 3.3$, $t = 6.6$, and $t = 9.9$ (upper to lower panels), with $\mathcal{A} = 5$. The doubly charged vortices dissolve into nonlinear structures and wave turbulence. From Shukla and Eliasson 2006.

and (58) was again solved numerically with the same initial condition as the one in Fig. 5, but with doubly charged vortices $s_1 = +2, s_2 = -2, s_3 = -2$, and $s_4 = +2$. The second row of panels in Fig. 6 reveals that the vortex pairs keep their identities for some time, while a quasi-1D density cavity is formed between the two vortex pairs. At a later stage, the four vortices dissolve into complicated nonlinear structures and wave turbulence. Hence, the nonlinear dynamics is very different between singly and multiply charged solitons, where only singly charged vortices are long lived and keep their identities.

VI. QUANTUM ELECTRON FLUID TURBULENCE

The statistical properties of quantum electron fluid turbulence and its associated electron transport properties at nanoscales in a quantum plasma have been investigated in both 2D and 3D by using the coupled NLS and Poisson equations (Shaikh and Shukla, 2007; 2008). It has been found that nonlinear couplings between the EPOs of different scale sizes

give rise to small-scale electron-density structures, while the ES potential cascades towards large scales. The total energy associated with the quantum electron plasma wave turbulence processes a nonuniversal spectrum that depends on the quantum electron coupling parameter.

To investigate 3D quantum electron plasma wave turbulence, we use the NLS-Poisson equations (Manfredi and Haas, 2001; Shukla, 2006; Shukla and Eliasson, 2006; Shaikh and Shukla, 2008)

$$i\sqrt{2H}\frac{\partial\Psi}{\partial t} + H\nabla^2\Psi + \varphi\Psi - |\Psi|^{4/3}\Psi = 0 \quad (69)$$

and

$$\nabla^2\varphi = |\Psi|^2 - 1, \quad (70)$$

were used, which govern the dynamics of nonlinearly interacting EPOs of different wavelengths. In Eqs. (69) and (70), the wave function is normalized by $\sqrt{n_0}$, the ES potential by $k_B T_{Fe}/e$, the time t by the electron plasma period ω_{pe}^{-1} , and the space \mathbf{r} by the electron Fermi-Thomas screening length $\lambda_{Fe} = V_{Fe}/\omega_{pe}$. Here $\sqrt{H} = \hbar\omega_{pe}/\sqrt{2}k_B T_{Fe}$ was introduced.

The nonlinear wave-wave coupling studies have been performed to investigate the multiscale evolution of a decaying 3D electron plasma wave turbulence, which is described by Eqs. (69) and (70). All fluctuations are initialized isotropically (no mean fields are assumed) with random phases and amplitudes in Fourier space, and are evolved in time by the integration of Eqs. (69) and (70) numerically. The initial isotropic turbulent spectrum was initially chosen close to k^{-2} , with random phases in all three directions. The choice of such (or even a flatter than k^{-2}) spectrum treats the turbulent fluctuations on an equal footing and avoids any influence on the dynamical evolution that may be due to the initial spectral nonsymmetry.

The properties of 3D electron plasma wave turbulence, composed of nonlinearly interacting EPOs, were studied for two specific physical systems, corresponding to dense plasmas in the next generation of laser-based plasma compression (LBPC) schemes (Malkin *et al.*, 2007), and in superdense astrophysical objects (Lai, 2001; Chabrier *et al.*, 2002; 2006; 2009; Harding and Lai, 2006) (e.g., white dwarfs). It is expected that, in LBPC schemes, the electron number density may reach 10^{27} cm^{-3} and beyond. Hence, we have $\omega_{pe} = 1.76 \times 10^{18} \text{ s}^{-1}$, $T_{Fe} = 1.7 \times 10^{-9} \text{ erg}$, $\hbar\omega_{pe} = 1.7 \times 10^{-9} \text{ erg}$, and $H = 1$, and the electron Fermi-Thomas screening length $\lambda_{Fe} = 0.1 \text{ \AA}$. On the other hand, in the core of white dwarf stars, we typically have $n_0 \sim 10^{30} \text{ cm}^{-3}$, yielding $\omega_{pe} = 5.64 \times 10^{19} \text{ s}^{-1}$, $T_{Fe} = 1.7 \times 10^{-7} \text{ erg}$ (0.1 MeV), $\hbar\omega_{pe} = 5.64 \times 10^{-8} \text{ erg}$, $H \approx 0.3$, and $\lambda_{Fe} = 0.025 \text{ \AA}$. The numerical solutions of Eqs. (69) and (70) for $H = 0.4$ and 0.01 (corresponding to $n_0 = 10^{27} \text{ cm}^{-3}$ and 10^{30} cm^{-3} , respectively) are shown in Fig. 7, which shows the electron number density and ES potential distributions in the (x, y, z) cube.

Figure 7 reveals that the electron-density distribution has a tendency to generate smaller length-scale structures, while the ES potential cascades towards larger scales. The coexistence of the small and larger scale structures in turbulence is a ubiquitous feature of various 3D turbulence systems. For example, in 3D hydrodynamic turbulence, the incompressible fluid admits two invariants, namely, the energy and the mean

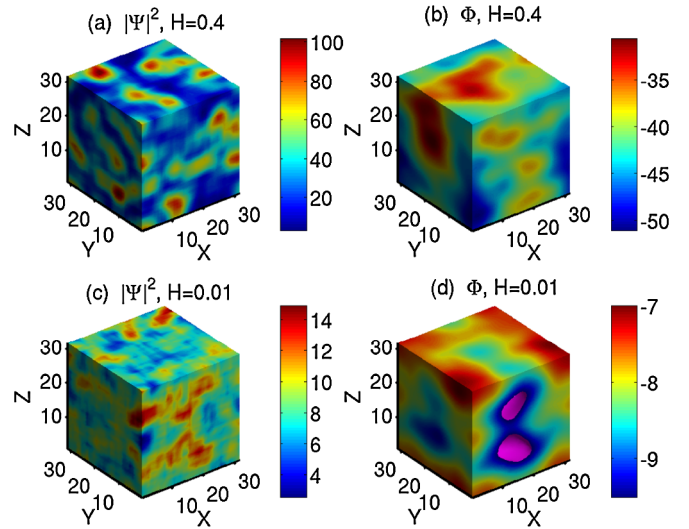


FIG. 7 (color online). Small-scale fluctuations in the electron density resulting from steady turbulence simulations, for $H = 0.4$ (a, b) and $H = 0.01$ (c, d). Forward cascades are responsible for the generation of small-scale fluctuations seen in (a) and (c). Large-scale structures are present in the ES potential, seen in (b) and (d), essentially resulting from an inverse cascade. From Shaikh and Shukla 2008.

squared vorticity. The two invariants, under the action of an external forcing, cascade simultaneously in turbulence, thereby leading to a dual cascade phenomena. In these processes, the energy cascades towards longer length scales, while the fluid vorticity transfers spectral power towards shorter length scales. Usually, a dual cascade is observed in a driven turbulence simulation, in which certain modes are excited externally through random turbulent forces in spectral space. The randomly excited Fourier modes transfer the spectral energy by conserving the constants of motion in k space. On the other hand, in freely decaying turbulence, the energy contained in the large-scale eddies is transferred to the smaller scales, leading to a statistically stationary inertial regime associated with the forward cascades of one of the invariants. Decaying turbulence often leads to the formation of coherent structures as turbulence relaxes, thus making the nonlinear interactions rather inefficient when they are saturated. The power spectrum exhibits an interesting feature in the 3D electron plasma system discussed here, unlike the 3D hydrodynamic turbulence (Kolmogorov, 1941a; 1941b; Lesieur, 1990; Frisch, 1995). Figure 8 shows the energy \mathcal{E}_k per vector wave number. For isotropic 3D turbulence, it is related to the energy E_k per scalar wave number as $E_k = 4\pi k^2 \mathcal{E}_k$ [see, e.g., Knight and Sirovich (1990)]. For $H = 0.4$, the spectrum per vector wave number is close to $\mathcal{E}_k \sim k^{-11/3}$ and hence yields the standard Kolmogorov power spectrum (Kolmogorov, 1941a; 1941b) $E_k \sim k^{-5/3}$. However, the spectrum is not universal but changes for different values of H . For 2D quantum electron fluid turbulence (Shaikh and Shukla, 2007) the spectral slope was more close to the Iroshnikov-Kraichnan power law (Iroshnikov, 1963; Kraichnan, 1965) $E_k \sim k^{-3/2}$. The origin of the differences in the observed spectral indices resides with the nonlinear character of the underlying plasma models, as nonlinear interactions in the 2D and 3D systems are governed typically by different nonlinear

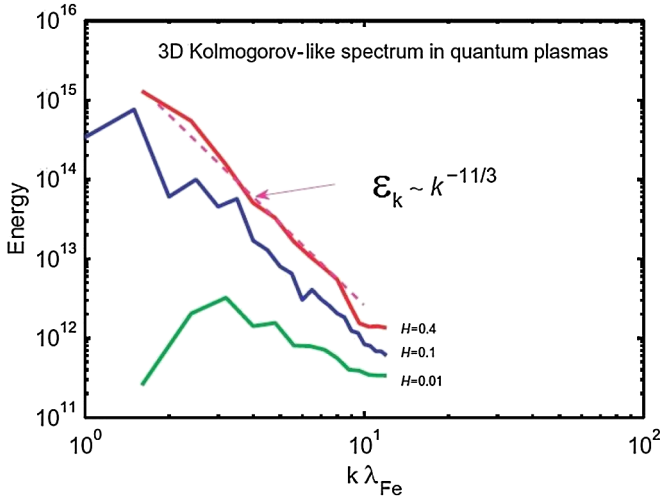


FIG. 8 (color online). Energy \mathcal{E}_k per vector wave number of 3D EPOs in the forward cascade regime. A Kolmogorov-like spectrum $\mathcal{E}_k \sim k^{-11/3}$ is observed for $H = 0.4$. The spectral index changes as a function of H . From Shaikh and Shukla 2008.

forces. The latter modify the spectral evolution of turbulent cascades to a significant degree. Physically, the flatness (or deviation from the $k^{-5/3}$ law) results from the short wavelength part of the EPOs spectrum, which is controlled by the quantum electron tunneling effect associated with the Bohm potential. The peak in the energy spectrum can be attributed to the higher turbulent power residing in the EPO potential, which eventually leads to the generation of larger scale structures, as the total energy encompasses both the electrostatic potential and electron-density components. In the dual cascade process, there is a delicate competition between the EPO dispersions caused by the statistical pressure law (giving the $k^2 V_{Fe}^2$ term, which dominates at longer scales) and the quantum Bohm force (giving the $\hbar^2 k^4 / 4m_e^2$ term, which dominates at shorter scales).

The electron diffusion in the presence of small and large-scale turbulent EPOs can be estimated in the following manner. An effective electron diffusion coefficient caused by the momentum transfer can be calculated from $D_{\text{eff}} = \int_0^\infty \langle \mathbf{P}(\mathbf{r}, t) \cdot \mathbf{P}(\mathbf{r}, t + t') \rangle dt'$, where \mathbf{P} is electron momentum and the angular bracket denotes spatial averages and the ensemble averages are normalized to unit mass. The effective electron diffusion coefficient D_{eff} essentially relates the diffusion processes associated with random translational motions of the electrons in nonlinear plasmonic fields. To measure the turbulent electron transport that is associated with the turbulent structures, D_{eff} is computed. It is observed that the effective electron diffusion is lower when the field perturbations are Gaussian. On the other hand, the electron diffusion increases rapidly with the eventual formation of large-scale structures, as shown in Fig. 9. The electron diffusion due to large-scale potential distributions in a quantum plasma dominates substantially, as shown by the solid curve in Fig. 9. Furthermore, in the steady state, nonlinearly coupled EPOs form stationary structures, and D_{eff} eventually saturates. Thus, remarkably an enhanced electron diffusion results primarily due to the emergence of large-scale potential structures.

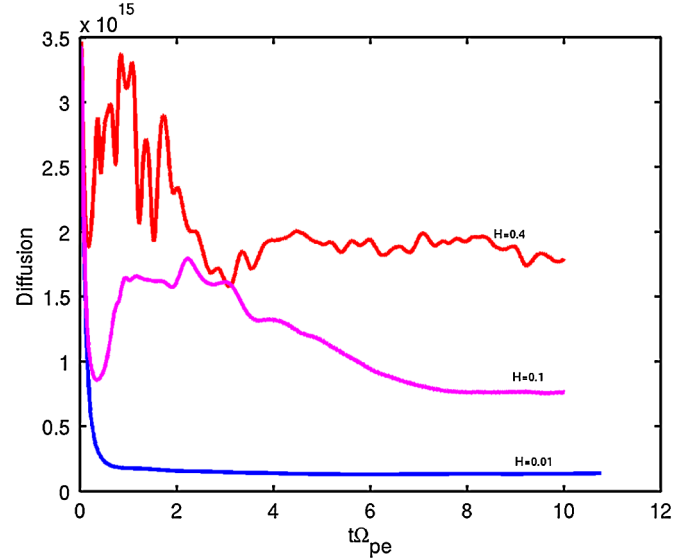


FIG. 9 (color online). Time evolution of the effective electron diffusion coefficient associated with the large-scale ES potential and the small-scale electron density, for $H = 0.4$, $H = 0.1$, and $H = 0.01$. Smaller values of H correspond to a small effective diffusion coefficient, which characterizes the presence of small-scale turbulent eddies that suppress the electron transport. From Shaikh and Shukla 2008.

VII. NONLINEARLY COUPLED EM AND ES WAVES

We now turn our attention to nonlinear interactions between large-amplitude EM and ES waves in a quantum plasma. Shukla and Stenflo (2006) considered nonlinear couplings between large-amplitude EM waves and finite amplitude electron and ion plasma waves, and presented nonlinear dispersion relations that exhibit stimulated Raman scattering (SRS), stimulated Brillouin scattering (SBS), and modulational instabilities. The work of Shukla and Stenflo (2006) has been further generalized by including thermal corrections to the ES waves (Stenflo and Shukla, 2009) and relativistic electron mass variations (Shukla and Eliasson, 2007) caused by EM waves in an unmagnetized quantum plasma.

A. Stimulated scattering instabilities

First, we present the governing equations for the HF-EM waves and the EM wave driven modified EPOs and IPOs. We have (Stenflo and Shukla, 2009)

$$\left(\frac{\partial^2}{\partial t^2} - c^2 \nabla^2 + \omega_{pe}^2 \right) \mathbf{A} + \omega_{pe}^2 \frac{n_1}{n_0} \mathbf{A} \approx 0 \quad (71)$$

for the HF-EM wave,

$$\left(\frac{\partial^2}{\partial t^2} + \omega_{pe}^2 - \frac{3}{5} V_{Fe}^2 \nabla^2 + \frac{\hbar^2}{4m_e^2} \nabla^4 \right) \frac{n_1}{n_0} = \frac{e^2}{2m_e^2 c^2} \nabla |\mathbf{A}|^2 \quad (72)$$

for the HF-EM wave pressure driven EPOs, and

$$\left(\frac{\partial^2}{\partial t^2} - C_{TF}^2 \nabla^2 + \frac{\hbar^2}{4m_e m_i} \nabla^4 \right) \frac{n_1}{n_0} = \frac{e^2}{2m_e m_i c^2} \nabla |\mathbf{A}|^2 \quad (73)$$

for the EM wave pressure driven modified IPOs without the ion thermal, ion viscoelastic relaxation, and ion viscosity

effects. Here $C_{TF} = (k_B T_{Fe}/m_i)^{1/2}$ and $n_1 (\ll n_0)$ is a small perturbation in the electron number density.

Following the standard procedure of the parametric instabilities (Yu *et al.*, 1974; Shukla *et al.*, 1981; Sharma and Shukla, 1983; Murtaza and Shukla, 1984; Shukla, 2006; Shukla and Eliasson, 2006), we can Fourier analyze (71)–(73) and combine the resultant equations to obtain the nonlinear dispersion relations

$$\omega^2 - \Omega_R^2 = -\frac{e^2 \omega_{pe}^2 k^2 |A_0|^2}{2m_e^2 c^2} \left(\frac{1}{D_+} + \frac{1}{D_-} \right) \quad (74)$$

and

$$\omega^2 - \Omega_B^2 = \frac{e^2 \omega_{pe}^2 k^2 |A_0|^2}{2m_e m_i c^2} \left(\frac{1}{D_+} + \frac{1}{D_-} \right), \quad (75)$$

for the driven EPOs and IPOs, respectively, which admit SRS, SBS, and modulational instabilities of the HF-EM pump (with the amplitude A_0) in a quantum plasma. Here $D_{\pm} = \pm 2\omega_0(\omega - \mathbf{k} \cdot \mathbf{V}_g) - k^2 c^2$, where $\mathbf{V}_g = \mathbf{k} c^2 / 2\omega_0$ is the group velocity of the HF-EM pump wave with the frequency $\omega_0 = (k_0^2 c^2 + \omega_{pe}^2)^{1/2}$, and

$$\Omega_R^2 = \omega_{pe}^2 + \frac{3}{5} k^2 V_{Fe}^2 + \frac{\hbar^2 k^4}{4m_e^2} \quad (76)$$

and

$$\Omega_B^2 = k^2 C_{TF}^2 + \frac{\hbar^2 k^4}{4m_e m_i}. \quad (77)$$

The growth rates of SRS and SBS instabilities (Shukla and Stenflo, 2006) are, respectively,

$$\gamma_R = \frac{\omega_{pe} e K |A_0|}{2\sqrt{2}\omega_0 \Omega_R m_e c}, \quad (78)$$

and

$$\gamma_B = \frac{\omega_{pe} e K |A_0|}{2\sqrt{2}\omega_0 \Omega_B m_e m_i c}. \quad (79)$$

The present results of SRS and SBS instabilities will help to identify the electrostatic spectral lines that are enhanced by the large-amplitude HF-EM pump wave in a quantum plasma.

B. Nonlinearly coupled intense EM and EPOs

We now consider nonlinear interactions between an arbitrary large-amplitude circularly polarized electromagnetic (CPEM) wave and nonlinear EPOs that are driven by the relativistic ponderomotive force (Shukla and Yu (1984) and Shukla *et al.* (1986) of the CPEM waves. Such an interaction gives rise to an envelope of the CPEM vector potential $\mathbf{A}_{\perp} = A_{\perp}(\hat{\mathbf{x}} + i\hat{\mathbf{y}}) \exp(-i\omega_0 t + ik_0 z)$, which obeys the NLS equation (Shukla and Eliasson, 2007)

$$2i\epsilon \left(\frac{\partial}{\partial t} + U_g \frac{\partial}{\partial z} \right) A_{\perp} + \frac{\partial^2 A_{\perp}}{\partial z^2} - \left(\frac{|\psi|^2}{\gamma} - 1 \right) A_{\perp} = 0, \quad (80)$$

where $\epsilon = \omega_0 / \omega_{pe}$, and the normalized (by $\sqrt{n_0}$) electron wave function ψ and the normalized (by $m_0 c^2 / e$) scalar potential are governed by, respectively,

$$iH_e \frac{\partial \psi}{\partial t} + \frac{H_e^2}{2} \frac{\partial^2 \psi}{\partial z^2} + (\phi - \gamma + 1)\psi = 0 \quad (81)$$

and

$$\frac{\partial^2 \phi}{\partial z^2} = |\psi|^2 - 1, \quad (82)$$

where m_0 is the rest mass of the electrons, $U_g = k_0 c / 2\omega_0$ is the group velocity, $H_e = \hbar \omega_{pe} / m_0 c^2$ is the ratio between the plasmonic energy density to the rest electron energy, and $\gamma = (1 + |A_{\perp}|^2)^{1/2}$ is the relativistic gamma factor due to the electron quiver velocity in the CPEM wave fields. The time and space variables are in units of the inverse electron plasma frequency (ω_{pe}^{-1}) and the electron skin depth $\lambda_e = c / \omega_{pe}$. The electron density and A_{\perp} are in units of n_0 and $m_0 c^2 / e$ (Shukla and Eliasson, 2007). The nonlinear coupling between intense CPEM waves and EPOs comes about due to the nonlinear current density, which is represented by the term $|\psi|^2 A_{\perp} / \gamma$ in Eq. (80). In Eq. (81), $1 - \gamma$ is the relativistic ponderomotive potential (Shukla and Yu, 1984; Shukla *et al.*, 1986). The latter arises from the averaging (over the CPEM wave period $2\pi / \omega_0$) of the relativistic advection and the nonlinear Lorentz force involving the electron quiver velocity and the CPEM wave electric and magnetic fields.

A relativistically strong EM wave in a classical electron-ion plasma is subject to SRS and modulational instabilities (McKinstry and Bingham, 1992). One can expect that these instabilities will be modified at the quantum scale by the dispersion effects caused by the tunneling of electrons through the quantum Bohm potential. The growth rate of the relativistic parametric instabilities in a dense quantum plasma in the presence of a relativistically strong CPEM pump wave can be obtained in a standard manner (Shukla *et al.*, 1986) by letting $\phi(z, t) = \phi_1(z, t)$, $A_{\perp}(z, t) = [A_0 + A_1(z, t)] \exp(-i\alpha_0 t)$, and $\psi(z, t) = [1 + \psi_1(z, t)] \exp(-i\beta_0 t)$, where A_0 is the large-amplitude CPEM pump and A_1 is the small-amplitude perturbation of the CPEM wave amplitude due to the nonlinear coupling between the CPEM waves and EPOs, i.e., $|A_1| \ll |A_0|$, and $\psi_1 (\ll 1)$ is the small-amplitude perturbation in the electron wave function. α_0 and β_0 are constant frequency shifts, determined from Eqs. (80) and (81) to be $\alpha_0 = (1/\gamma_0 - 1)/(2\epsilon)$, and $\beta_0 = (1 - \gamma_0)/H_e$, where $\gamma_0 = (1 + |A_0|^2)^{1/2}$. The first-order perturbations in the electromagnetic vector potential and the electron wave function are expanded into their respective sidebands as $A_1(z, t) = A_+ \exp(iKz - i\Omega t) + A_- \exp(-iKz + i\Omega t)$ and $\psi_1(z, t) = \psi_+ \exp(iKz - i\Omega t) + \psi_- \exp(-iKz + i\Omega t)$, while the potential is expanded as $\phi(z, t) = \hat{\phi} \exp(iKz - i\Omega t) + \hat{\phi}^* \exp(-iKz + i\Omega t)$, where Ω and K are the normalized frequency and the normalized wave number of the EPOs, respectively. Inserting the above mentioned Fourier ansatz into Eqs. (80)–(82), linearizing the resultant system of equations, and sorting into equations for different Fourier modes, one obtains the nonlinear dispersion relation (Shukla and Eliasson, 2007)

$$1 + \left(\frac{1}{\tilde{D}_+} + \frac{1}{\tilde{D}_-} \right) \left(1 + \frac{K^2}{D_L} \right) \frac{|A_0|^2}{2\gamma_0^3} = 0, \quad (83)$$

where $\tilde{D}_{\pm} = \pm 2\epsilon(\Omega - KU_g) - K^2$ and $D_L = 1 - \epsilon^2 + H_e^2 K^4 / 4$. One notes that $D_L = 0$ yields the linear dispersion relation $\Omega^2 = 1 + H_e^2 K^4 / 4$ for the EPOs in a dense quantum plasma (Pines, 1961). For $H_e \rightarrow 0$, we recover from Eq. (83) the nonlinear dispersion relation for relativistically large-amplitude EM waves in a classical electron plasma

(McKinstrie and Bingham, 1992). The dispersion relation (83) governs stimulated Raman backward and forward scattering instabilities, as well as the modulational instability. In the long-wavelength limit $U_g \ll 1$, $\epsilon \approx 1$ one can use the ansatz $\Omega = i\Gamma$, where the normalized (by ω_{pe}) growth rate $\Gamma \ll 1$, and obtain from Eq. (83) the growth rate $\Gamma = (1/2)|K|\{(|A_0|^2/\gamma_0^3)[1 + K^2/(1 + H_e^2 K^4/4)] - K^2\}^{1/2}$ of the modulational instability. For $|K| < 1$ and $H_e < 1$, the linear growth rate is only weakly depending on the quantum parameter H_e .

The quantum dispersion effects on nonlinearly coupled CPEM and EPOs can be studied by considering a steady-state structure moving with a constant speed U_g . Inserting the ansatz $A_\perp = W(\xi) \exp(-i\Omega_e t)$, $\psi = P(\xi) \exp(ik_e x - i\omega_e t)$, and $\phi = \phi(\xi)$ into Eqs. (80)–(82), where $\xi = z - U_g t$, $k_e = U_g/H_e$, and $\omega_e = U_g^2/2H_e$, and where $W(\xi)$ and $P(\xi)$ are real, one obtains from Eqs. (80)–(82) the coupled system of equations (Shukla and Eliasson, 2007)

$$\frac{\partial^2 W}{\partial \xi^2} + \left(\lambda - \frac{P^2}{\gamma} + 1\right)W = 0, \tag{84}$$

$$\frac{H_e^2}{2} \frac{\partial^2 P}{\partial \xi^2} + (\phi - \gamma + 1)P = 0, \tag{85}$$

where $\gamma = (1 + W^2)^{1/2}$ and

$$\frac{\partial^2 \phi}{\partial \xi^2} = P^2 - 1, \tag{86}$$

with the boundary conditions $W = \Phi = 0$ and $P^2 = 1$ at $|\xi| = \infty$. In Eq. (84), $\lambda = 2\epsilon\Omega_e$ represents a nonlinear frequency shift of the CPEM wave. In the limit $H_e \rightarrow 0$, one has from Eq. (85) $\phi = \gamma - 1$, where $P \neq 0$, and one recovers the classical (nonquantum) case of the relativistic solitary waves in a cold plasma (Marburger and Tooper, 1975).

The system of equations (84)–(86) admits a Hamiltonian

$$Q_H = \frac{1}{2} \left(\frac{\partial W}{\partial \xi}\right)^2 + \frac{H_e^2}{2} \left(\frac{\partial P}{\partial \xi}\right)^2 - \frac{1}{2} \left(\frac{\partial \phi}{\partial \xi}\right)^2 + \frac{1}{2} (\lambda + 1)W^2 + P^2 - \gamma P^2 + \phi P^2 - \phi = 0, \tag{87}$$

where the boundary conditions $\partial/\partial \xi = 0$, $W = \phi = 0$, and $|P| = 1$ at $|\xi| = \infty$ have been used.

Numerical solutions of the quasistationary system (84)–(86) are shown in Figs. 10 and 11, while time-dependent solutions of Eqs. (80)–(82) are displayed in Figs. 12 and 13. Here parameters were used that are representative of the next generation of LBPC schemes (Azechi *et al.*, 2006; Malkin *et al.*, 2007). The formula (Shukla *et al.*, 1986) $eA_\perp/mc^2 = 6 \times 10^{-10} \lambda_s \sqrt{I}$ will determine the normalized vector potential, provided that the CPEM wavelength λ_s (in microns) and the CPEM wave intensity I (in W/cm²) are known. It is expected that in LBPC schemes, the electron number density n_0 may reach 10^{27} cm⁻³ and beyond, and the peak values of eA_\perp/mc^2 may be in the range of 1–2 (e.g., for focused EM pulses with $\lambda_s \sim 0.15$ nm and $I \sim 5 \times 10^{27}$ W/cm²). For $\omega_{pe} = 1.76 \times 10^{18}$ s⁻¹, one has $\hbar\omega_{pe} = 1.76 \times 10^{-9}$ erg and $H_e = 0.002$, since $mc^2 = 8.1 \times 10^{-7}$ erg. The electron skin depth is $\lambda_e \sim 1.7$ Å. On the other hand, a higher value of $H_e = 0.007$ is achieved for $\omega_{pe} = 5.64 \times 10^{18}$ s⁻¹. Thus, the numerical solutions below, based on these two values of H_e ,

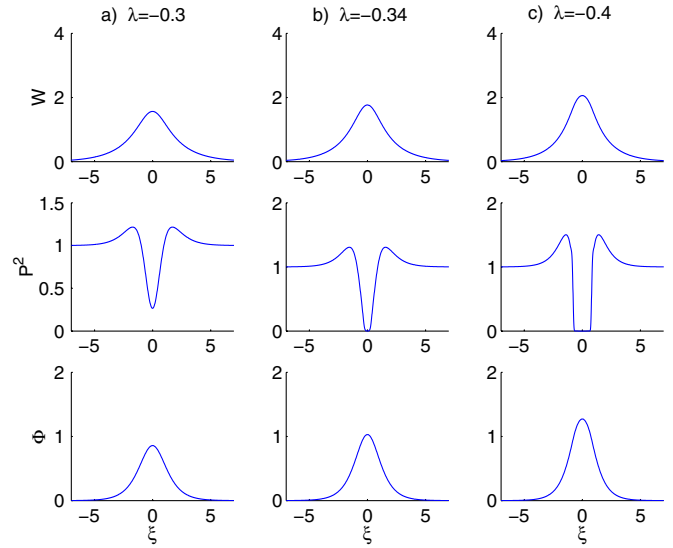


FIG. 10 (color online). The profiles of the CPEM vector potential W (top row), the electron number density P^2 (middle row), and the scalar potential Φ (bottom row) for $\lambda = -0.3$ (left column), $\lambda = -0.34$ (middle column), and $\lambda = -0.4$ (right column), with $H_e = 0.002$. From Shukla and Eliasson 2007.

have focused on scenarios that are relevant for the next generation intense laser-solid density plasma interaction experiments (Malkin *et al.*, 2007).

Figures 10 and 11 exhibit numerical solutions of Eqs. (84)–(86) for $H_e = 0.002$ and 0.007 . The nonlinear boundary value problem was solved with the boundary conditions $W = \phi = 0$ and $P = 1$ at the boundaries at $\xi = \pm 10$. The solitary envelope pulse is composed of a single maximum of the localized vector potential W and a local depletion

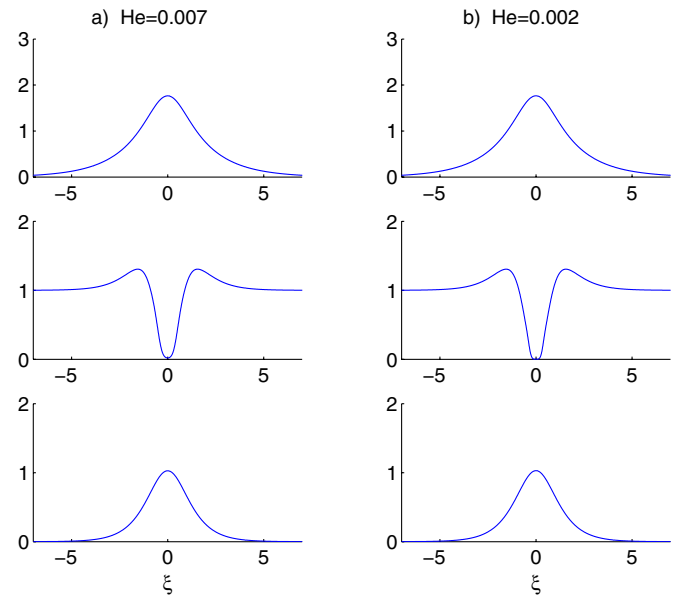


FIG. 11 (color online). The profiles of the CPEM vector potential W (top row), the electron number density P^2 (middle row), and the scalar potential Φ (bottom row) for $H_e = 0.007$ (left column) and $H_e = 0.002$ (right column), with $\lambda = -0.34$. From Shukla and Eliasson 2007.

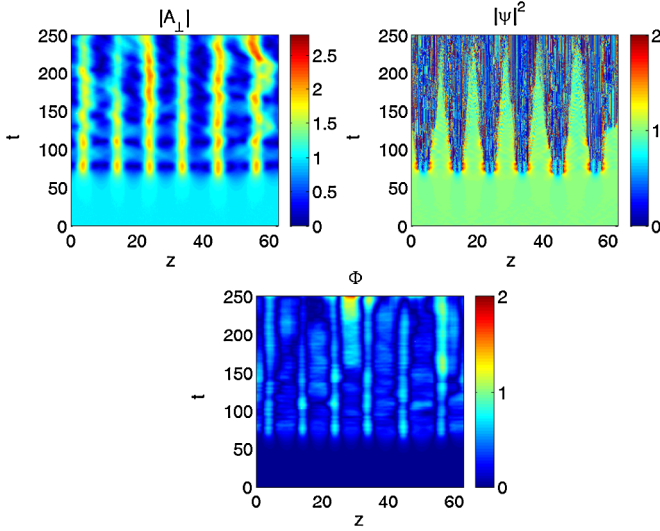


FIG. 12 (color online). The dynamics of the CPWM vector potential A_{\perp} and the electron number density $|\psi|^2$ (upper panels) and of the electrostatic potential Φ (lower panel) for $H_e = 0.002$. From Shukla and Eliasson 2007.

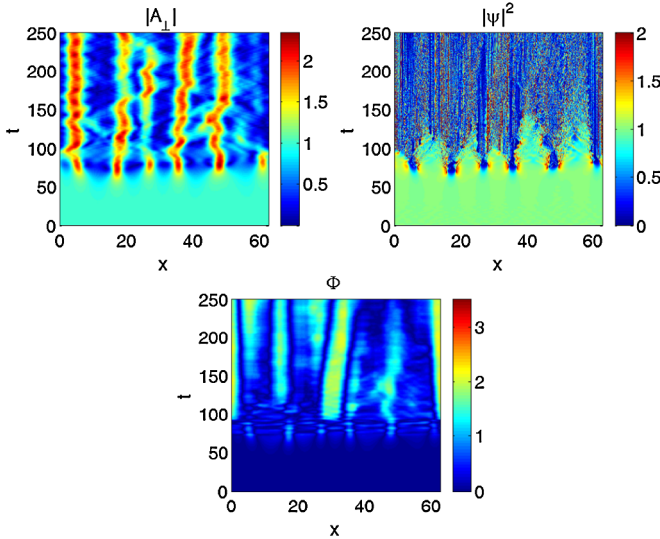


FIG. 13 (color online). The dynamics of the CPWM vector potential A_{\perp} and the electron number density $|\psi|^2$ (upper panels) and the electrostatic potential ϕ (lower panel) for $H_e = 0.007$. From Shukla and Eliasson 2007.

of the electron density P^2 , and a localized positive potential ϕ at the center of the solitary pulse. The latter has a continuous spectrum in λ , where larger values of negative λ are associated with larger-amplitude solitary EM pulses. At the center of the solitary EM pulse, the electron density is partially depleted, as in Fig. 10(a), and for larger amplitudes of the EM waves one has a stronger depletion of the electron density, as shown in panels Figs. 10(a) and 10(b). For cases where the electron density goes to almost zero in the classical case (Marburger and Tooper, 1975), one important quantum effect is that the electrons can tunnel through the depleted density region. This is seen in Fig. 11, where the electron density remains nonzero for $H_e = 0.007$ in Fig. 11(a), while the density shrinks to zero for $H_e = 0.002$ in Fig. 11(b).

Figures 12 and 13 show numerical simulation results of Eqs. (80)–(82) for the long-wavelength limit characterized by $\omega_0 \approx 1$ and $V_g \approx 0$. As initial conditions, we used an EM pump with a constant amplitude $A_{\perp} = A_0 = 1$ and a uniform plasma density $\psi = 1$, together with a small-amplitude noise (random numbers) of order 10^{-2} added to A_{\perp} to give a seeding any instability. The numerical results are shown in Figs. 12 and 13 for $H_e = 0.002$ and 0.007, respectively. In both cases, we see an initial linear growth phase and a wave collapse at $t \approx 70$, in which almost all of the CPWM wave energy is contracted into a few well separated large amplitude, localized CPWM envelopes, associated with an almost complete depletion of the electron density at the center of the CPWM wave packet, and a large-amplitude positive electrostatic potential. One can see that there are more complex dynamics of localized CPWM wave packets for $H_e = 0.007$, shown in Fig. 13, in comparison with $H_e = 0.002$, shown in Fig. 12, where the wave packets are almost stationary when they are fully developed.

VIII. MAGNETIZED QUANTUM PLASMAS

Magnetized quantum plasmas occur in white dwarf stars and on the surface of magnetized stars (e.g., magnetars) where degenerate electrons could be ultrarelativistic, but the ions are in a nondegenerate state. How strong magnetic fields in dense stars come about is still unresolved, although there are evidence of the strong magnetization of dense plasmas in astrophysical environments. In dense magnetized plasmas, one has to account for the Lorentz force and the Landau quantization effect (Landau and Lifshitz, 1998a), and develop the appropriate quantum Hall-magnetohydrodynamics (Q-HMHD) equations starting from the Wigner-Maxwell equations. We stress, however, that the Q-HMHD equations discussed here do not capture the particular physics of the quantized Hall resistance $R_k = \hbar/\nu e^2$ (Klitzing *et al.*, 1980). In semiconductors with 2D electrons, the latter is associated with the quantized electron density $n_q = \nu e B_0/\hbar c$ at high magnetic fields and low temperature, where ν is an integer, appearing in the electron current ($-en_q \mathbf{u}_d$) flowing through a conductor. Here $\mathbf{u}_d = (c/B_0^2) \mathbf{E} \times \mathbf{B}_0$ is the cross field electron drift associated with the space charge electric field \mathbf{E} that results from the motion of electrons by the Lorentz force. The Ohm's law, in turn, determines the von Klitzing resistance, which is independent of the magnetic field.

A. Landau quantization

In a strong magnetic field $\hat{\mathbf{z}}B_0$, where $\hat{\mathbf{z}}$ is the unit vector along the z axis in a Cartesian coordinate system, and B_0 is the strength of the external magnetic field, the electron motion in a plane perpendicular to the magnetic field direction is quantized (Landau and Lifshitz, 1998b). The electron energy level is determined by the nonrelativistic limit by (Landau and Lifshitz, 1998b; Tsintsadze, 2010)

$$\mathcal{E}_e^{l,\sigma} = \frac{p_z^2}{2m_e} + (2l + 1 + \sigma)\mu_B B_0, \quad (88)$$

where p_z is the electron momentum in the z direction, l is the orbital angular number ($l = 0, 1, 2$), and $\sigma = \pm 1$ represents the spin orientation. For $\sigma = -1$, we have from Eq. (88)

$$\mathcal{E}_e^l = \frac{p_z^2}{2m_e} + \hbar\omega_{ce}, \quad (89)$$

where $\omega_{ce} = eB_0/m_e c$ is the electron gyrofrequency. Accordingly, the Fermi-Dirac electron distribution is Tsintsadze (2010)

$$F_D(p_z, l) \propto \frac{1}{1 + \exp[(E_z + \hbar\omega_{ce} - \mu_e)/k_B T_e]}, \quad (90)$$

where $E_z = (m_e/2)v_z^2$ is the parallel (to $\hat{\mathbf{z}}$) kinetic energy of degenerate electrons.

Assuming that $|\omega_{ce} - \mu_e| \gg k_B T_e$, one can approximate the Fermi-Dirac distribution function by the Heaviside step function $H(\mu_e - \mathcal{E}_e^l)$, which is equal to 1 for $\mu_e = E_{Fe} = k_B T_{Fe} = (p_F^2/2m_e)^{1/2} > \mathcal{E}_e^l$ and 0 for $E_{Fe} < \mathcal{E}_e^l$, where $p_F = m_e v_{TF}$. The equilibrium electron number density is (Tsintsadze, 2010)

$$n_e = \frac{p_F^3}{2\pi^2 \hbar^3} \left[\Gamma_B + \frac{2}{3}(1 - \Gamma_B)^{3/2} \right], \quad (91)$$

where $\Gamma_B = \hbar\omega_{ce}/k_B T_{Fe}$. The current carried by degenerate electrons in a magnetized quantum plasma is $-en_e \mathbf{u}_d$, which yields the plasma resistivity $R_s = en_e c/B_0$.

B. ESOs and EM waves

In a magnetized quantum plasma, there are finite density perturbations associated with high-frequency electrostatic electron-Bernstein (EB) waves and elliptically polarized EM waves (EP-EM waves) that propagate across the magnetic field direction $\hat{\mathbf{z}}$. Furthermore, the CPEM wave propagating along $\hat{\mathbf{z}}$ are not associated with any density perturbation.

The dispersion relation for the EB waves in a Fermi-Dirac distributed plasma is in the ultracold limit (Eliasson and Shukla, 2008b)

$$1 + \frac{3\omega_{pe}^2}{\omega_{ce}^2} \int_0^\pi d\theta \frac{\sin(\Omega\theta)\sin(\theta)\sin(\xi_e) - \xi_e \cos(\xi_e)}{\xi_e^3} = 0, \quad (92)$$

where $\Omega = \omega/\omega_{ce}$, $\xi_e = (2k_\perp^2 \rho_{Fe}^2) \cos(\theta/2)$, and $\rho_{Fe} = V_{Fe}/\omega_{pe}$ is the gyroradius of degenerate electrons. Solutions of Eq. (92) are plotted in Fig. 14 for the case $\omega_{UH} = 4\omega_{ce}$, where $\omega_{UH} = (\omega_{pe}^2 + \omega_{ce}^2)^{1/2}$ is the upper-hybrid (UH) resonance frequency. In the long-wavelength limit (viz. $k_\perp^2 \rho_{Fe}^2 \ll 1$), Eq. (92) yields

$$\omega^2 = \omega_{UH}^2 + \frac{3}{5} \frac{\omega_{pe}^2 k_\perp^2 V_{Fe}^2}{\omega^2 - 4\omega_{ce}^2}, \quad (93)$$

where k_\perp is the perpendicular (to $\hat{\mathbf{z}}$) component of the propagation wave vector. For $\omega \approx \omega_H$, Eq. (93) reveals that the propagating UH waves have positive (negative) group dispersion in plasmas with $\omega_{pe} > \sqrt{3}\omega_{ce}$ ($\omega_{pe} < \sqrt{3}\omega_{ce}$).

Furthermore, the refractive index N_x for the EP-EM waves propagating along the x axis (which is orthogonal to $\hat{\mathbf{z}}$) is (Shukla, 2007)

$$N_x = \frac{k_x^2 c^2}{\omega^2} = 1 - \frac{\omega_{pe}^2}{\omega^2} - \frac{\omega_{pe}^2 \omega_{ce}^2 [1 + \eta(\alpha) k_x^2 \lambda_b^2]}{\omega^2 [\omega^2 - \omega_{UH}^2 + k_x^2 V_{Fe}^2 (1 + k_x^2 \lambda_q^2)]}, \quad (94)$$

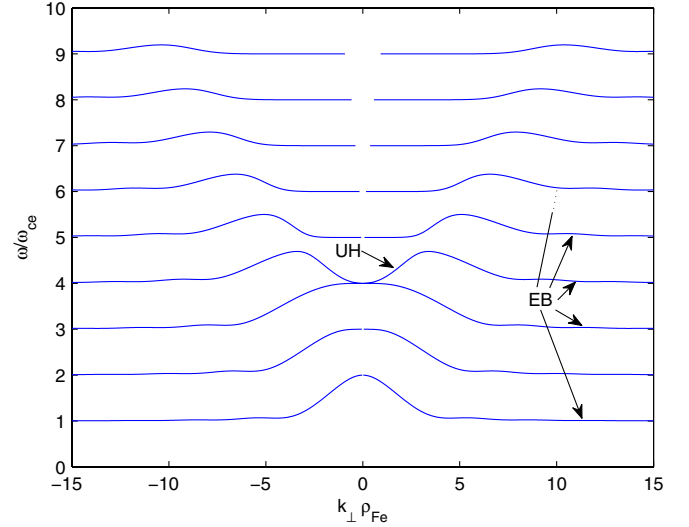


FIG. 14 (color online). Dispersion curves for EB waves in a Fermi-Dirac distributed plasma, showing several EB modes and the UH branch. From Eliasson and Shukla 2008b.

where k_x is the x component of the propagation wave vector, $\lambda_q^2 = \hbar^2/4m_e V_{Fe}^2$, $\lambda_b = \sqrt{\hbar/2m_e \omega_{ce}}$, $\eta(\alpha) = 2 \tanh(\alpha)$, and $\alpha = \mu_B B_0/k_B T_{Fe}$. Several comments are in order. First, we note that the electron spin-1/2 effect enhances the electron gyrofrequency by a factor of $(1 + \eta k_x^2 \lambda_b^2)^{1/2}$ in the numerator of the third term on the right-hand side of Eq. (94). Second, the quantum Bohm force produces a dispersion term $\hbar k^4/4m_e^2$ in the denominator of the third term in Eq. (94). Third, in the limit of vanishing \hbar , Eq. (95) correctly reproduces the EP-EM wave dispersion relation. Furthermore, Eq. (94) reveals that the cutoff frequencies (at $k_x = 0$) in dense magnetoplasmas are

$$\omega = \omega_{\pm} = \frac{1}{2} [(4\omega_{pe}^2 + \omega_{ce}^2)^{1/2} \pm \omega_{ce}], \quad (95)$$

which are the same as the cutoffs of the X(upper sign) and Z(lower sign) mode waves in a classical plasma (Chen, 2006). Short-wavelength electromagnetic propagation in magnetized quantum plasmas, including quantum electrodynamic effects, has also been considered by Lundin *et al.* (2007).

The vector representation of spinning quantum particles in the quantum theory was first introduced by Takabayasi (1955) who developed the QHD involving the evolution of the quantum particle spin. The idea of Takabayasi has been further elaborated by Brodin *et al.* (2010) in the context of the spin contribution to the ponderomotive force of the magnetic field-aligned CPEM waves in a quantum magnetoplasma. In fact, by using the nonrelativistic electron momentum equation (Brodin *et al.*, 2010)

$$m_e \left(\frac{\partial}{\partial t} + \mathbf{u}_e \cdot \nabla \right) \mathbf{u}_e = -e \left(\mathbf{E} + \frac{1}{c} \mathbf{u}_e \times \mathbf{B} \right) - \frac{g}{\hbar} \mu_B \nabla (\mathbf{B} \cdot \mathbf{s}), \quad (96)$$

and the spin evolution equation

$$\left(\frac{\partial}{\partial t} + \mathbf{u}_e \cdot \nabla \right) \mathbf{s} = \frac{g \mu_B}{\hbar} (\mathbf{B} \times \mathbf{s}), \quad (97)$$

together with Ampère's law and suitable Maxwell's equation [incorporating the electron magnetization current, $\mathbf{J}_M = -(4\pi/c)(g \mu_B/\hbar) \nabla \times (n_e \times \mathbf{s})$, due to the electron

1/2-spin effect], where \mathbf{s} is the spin angular momentum, with its absolute value $|\mathbf{s}| = s_0 = \hbar/2$. The quantity $g = 2.0023192$ is the electron Gaunt factor (sometimes called the g factor or spectroscopic splitting factor). The value $g = 2$ is predicted from Dirac's relativistic theory of the electron, while the correction to this value comes from the quantum electrodynamics (Kittel, 1996; Bransden and Joachain, 2000).

Brodin *et al.* (2010) derived the spin-ponderomotive force $\hat{\mathbf{z}}F_s$ for the CPEM wave, where

$$F_s = \mp \frac{g^2 \mu_B^2 s_0}{m_e^2 \hbar^2 (\omega \pm \omega_g)} \left[\frac{\partial}{\partial z} - \frac{k}{(\omega \pm \omega_g)} \frac{\partial}{\partial t} \right] |\mathbf{B}_w|^2. \quad (98)$$

Here $\omega_g = g \mu_B B_0 / \hbar$ the spin-precession frequency and \mathbf{B}_w is the CPEM wave magnetic field. The spin-ponderomotive force comes from the averaging of the third term in (99) over the CPEM wave period $2\pi/\omega$. The CPEM wave frequency ω is determined from the dispersion relation

$$\left(1 \mp \frac{\omega_\mu}{\omega \pm \omega_g} \right) N_z^2 = 1 - \frac{\omega_{pe}^2}{\omega(\omega \pm \omega_{ce})}, \quad (99)$$

where $N_z = k_z c / \omega$, k_z is the component of the wave vector \mathbf{k} along the z axis, $\omega_\mu = g^2 s_0 / 4m_e \lambda_e^2$, $\lambda_e = c / \omega_{pe}$, and the $+$ ($-$) represents the left-hand (right-hand) circular polarization. The ω_μ term in Eq. (99) is associated with the electron spin evolution. It changes the dispersion properties of the magnetic field-aligned EM electron-cyclotron waves in a quantum magnetoplasma. Furthermore, the spin-ponderomotive force induces a strong spin polarization of a quantum magnetoplasma.

It should be noted that there is also a standard nonstationary ponderomotive force ($\hat{\mathbf{z}}F_e$) (Karpman and Washimi, 1977) of the CPEM waves arising from the averaging of the nonlinear Lorentz force term $-(e/m_e c) \hat{\mathbf{z}} \cdot (\mathbf{u}_e \times \mathbf{B}_w)$ over the CPEM wave period $2\pi/\omega$, where

$$F_e = - \frac{e^2}{2m_e^2 \omega (\omega \pm \omega_{ce})} \left(\frac{\partial}{\partial z} \pm \frac{k_z \omega_{ce}}{\omega (\omega \pm \omega_{ce})} \frac{\partial}{\partial t} \right) |\mathbf{E}_w|^2, \quad (100)$$

and $\mathbf{E}_w = (\omega/k_z c) \mathbf{B}_w$ is the CPEM wave electric field.

C. Q-HMHD equations

To a first approximation, the dynamics of low-phase speed (in comparison with the speed of light in vacuum) electromagnetic waves in dense magnetoplasmas is modeled by the Q-HMHD equations. The latter include the inertialess electron momentum equation

$$0 = -en_e \left(\mathbf{E} + \frac{1}{c} \mathbf{u}_e \times \mathbf{B} \right) - \nabla P_C, \quad (101)$$

where the quantum Bohm and quantum spin forces are supposed to be unimportant on the characteristic scale length of present interest. The degenerate electrons are coupled with the nondegenerate ions through the EM forces. The ion dynamics is governed by the ion continuity equation (43) and the momentum equation

$$m_i n_i \frac{d\mathbf{u}_i}{dt} = n_i e \left(\mathbf{E} + \frac{1}{c} \mathbf{u}_i \times \mathbf{B} \right), \quad (102)$$

where $d/dt = (\partial/\partial t) + \mathbf{u}_i \cdot \nabla$. For simplicity, we have assumed here that $\tau_m \partial/\partial t \ll 1$ and $\partial \mathbf{u}_i / \partial t \gg (\eta/\rho_i) \nabla \cdot \nabla \mathbf{u}_i + \rho_i^{-1} (\xi + \eta/3) \nabla (\nabla \cdot \mathbf{u}_i)$. The EM fields are given by Faraday's law

$$\frac{\partial \mathbf{B}}{\partial t} = -c \nabla \times \mathbf{E}, \quad (103)$$

and Maxwell's equation

$$\nabla \times \mathbf{B} = \frac{4\pi e}{c} (n_i \mathbf{u}_i - n_e \mathbf{u}_e) + \frac{1}{c} \frac{\partial \mathbf{E}}{\partial t}. \quad (104)$$

By using Eq. (101), we can eliminate the electric field \mathbf{E} from Eq. (102), obtaining for a quasineutral ($n_e = n_i = n$) quantum magnetoplasma

$$m_i n \frac{d\mathbf{u}_i}{dt} = -\nabla P_C - \frac{1}{8\pi} \nabla \mathbf{B}^2 + \frac{(\mathbf{B} \cdot \nabla) \mathbf{B}}{4\pi}, \quad (105)$$

where we have used Eq. (104) without the displacement current (the last term on the right-hand side) for the low-phase speed (in comparison with c) EM wave phenomena. By using the electric field from Eq. (102), we can write Eq. (103) as

$$\frac{\partial \mathbf{B}}{\partial t} = \nabla \times (\mathbf{u}_i \times \mathbf{B}) - \frac{m_i c}{e} \frac{d\mathbf{u}_i}{dt}. \quad (106)$$

Equations (43), (105), and (106) are the desired Q-HMHD equations for studying the linear and nonlinear dispersive EM waves, as well as new aspects of 3D quantum fluid turbulence in a quantum magnetoplasma with degenerate electrons having Chandrasekhar's pressure law. However, when the Landau quantization effect in a very strong magnetic field is accounted for, one can replace P_C by the appropriate pressure law (Eliesser *et al.*, 2005)

$$P_L = \frac{4eB_0(2m_e)^{1/2} E_F^{3/2}}{3(2\pi)^2 \hbar^2 c} \left[1 + 2 \sum_{l=1}^{l_m} \left(1 - \frac{l\hbar\omega_{ce}}{k_B T_{Fe}} \right)^{3/2} \right], \quad (107)$$

where the value of l_m is fixed by the largest integer that satisfies $k_B T_{Fe} - l\hbar\omega_{ce} \leq 0$.

IX. SUMMARY AND OUTLOOK

In this Colloquium paper, we described the essential physics of quantum plasmas with degenerate electron fluids. We reviewed the properties of quantum plasmas and quantum models that describe the salient features of linear and nonlinear ES and EM waves. Specifically, the focus of the present Colloquium article has been on developing the model nonlinear equations that depict new features of nonlinear waves and quantum electron fluid turbulence at nanoscales. Numerical simulations of the NLS-Poisson equations reveal quasistationary, localized structures in the form of one-dimensional electron-density holes (dark solitons) and 2D quantum electron vortices. These localized quantum structures, which are associated with a local depletion of the electron density and a positive electrostatic potential, arise due to a balance between the nonlinear and dispersion effects involved in the dynamics of nonlinearly interacting EPOs. In 2D, there exist a class of quantum electron vortices of different excited states (charge states). Furthermore, numerical simulations also depict that the time-dependent NLS-Poisson equations exhibit stability of a dark soliton in

one-space dimension. In 2D, the dark solitons of the first excited state are stable and the preferred nonlinear state is in the form of quantum vortex pairs of different polarities. The one-dimensional dark soliton and singly charged 2D quantum vortices are thus long-lived nonlinear structures at nanoscales. Also presented are theoretical and computer simulation studies of nonlinearly coupled intense EM waves and EPOs in an unmagnetized quantum plasma. We reported new classes of stimulated scattering instabilities of EM waves and trapping of intense EM waves in a quantum electron-density hole.

It should be noted that inclusion of nondegenerate ion dynamics gives rise to new features to linear and nonlinear IPOs (Haas *et al.*, 2003; Eliasson and Shukla, 2008a). Furthermore, nonlinear equations governing the coupling between the dispersive Langmuir and ion-acoustic waves, which are known as the quantum Zakharov equations (Garcia *et al.*, 2005; Misra *et al.*, 2008; Haas and Shukla, 2009; Simpson *et al.*, 2009), admit periodic, quasiperiodic, chaotic, and hyperchaotic states (Misra *et al.*, 2008), in addition to arresting the Langmuir wave collapse (Haas and Shukla, 2009; Simpson *et al.*, 2009) due to quantum dispersion effects. There may also emerge new aspects of nonlinear EPOs and IPOs when the particle trapping (Jovanovic and Fedele, 2007) in the strong wave potential is included. Here one has to obtain nonlinear solutions of nonstationary Wigner-Poisson equations, which might reveal a modified (by the electrostatic wave potential) Fermi-Dirac electron distribution function. Furthermore, there is a scope for studying the collective nonlinear response of correlated Coulomb electron systems at finite temperatures by means of kinetic theory concepts (Domps *et al.*, 1997) to incorporate collisions and Green's function methods originally developed by Baym and Kadanoff (1961). We note that the Baym-Kadanoff approach has been used by Kwong and Bonitz (2000) to investigate the dielectric properties (viz. inverse dielectric function and dynamic structure factor) of linear EPOs in a correlated electron gas. Furthermore, the ion-ion dynamic structure factor, which contains a wealth of information about ions including structure and low-frequency collective modes in a dense quantum plasma, has been studied by Murillo (2010).

The field of the nonlinear quantum plasma physics is vibrant, and its potential applications rest on our complete understanding of numerous collective processes in compact astrophysical objects, as well as in the next generation of intense laser-solid density plasma experiments and in the plasma-assisted nanotechnology (e.g., quantum free-electron laser devices, quantum diodes, metallic nanostructures, nanowires, nanotubes, etc.). However, nonlinear quantum models presented in this Colloquium paper have to be further improved and generalized by including the effects of the electron-exchange interactions, strong electron-electron correlations, equilibrium inhomogeneities of the magnetic field, and the plasma density, as well as fully relativistic and Landau quantization effects in a nonuniform quantum magnetoplasma. We also have to understand the features of quantum oscillations of electrons and possible formation of bound states of electrons in the presence of an external magnetic field. For this purpose, we have to calculate the interaction potential among highly correlated electrons and use molecular dynamic simulations to demonstrate attraction

among electrons due to collective wave-quantum particle interactions that give rise to Cooper's pairing of degenerate electrons. Cooper's pairing of electrons could possibly provide a scenario of superconducting behavior of a quantum plasma. Furthermore, 2D system composed of electron clusters at finite temperature exhibits Wigner Coulomb crystallization (Egger *et al.*, 1999; Filinov *et al.*, 2001). The latter has been investigated by means of Monte Carlo simulations based on a quantum Hamiltonian with parabolic confining and Coulomb interaction potentials. In a nonuniform quantum magnetoplasma, we have ES drift waves (Shokri and Rukhadze, 1999; Ali *et al.*, 2007; and Saleem *et al.*, 2008), which can drastically affect the cross field electron transport. For applications to plasma-assisted nanotechnology devices (e.g., nonlinear electrostatic and electromagnetic surface waves in metallic nanostructure-devices, photonic band gap, and x-ray optical systems, quantum x-ray free-electron laser systems), one must also study nonlinear collective processes by including both the electron spin 1/2 and quantum electron tunneling effects on an equal footing. Finally, the localization of coupled ES and EM waves due to nonlinear quantum effects in a nonuniform quantum magnetoplasma with an arbitrary electron pressure degeneracy should provide clues to the origin of very intense x-rays (Coe *et al.*, 1978) and gamma rays (Hurley *et al.*, 2005) from both astrophysical and laboratory plasmas.

ACKNOWLEDGMENTS

This research was supported by the Deutsche Forschungsgemeinschaft through Project No. SH21/3-1 of the Research Unit 1048, and by the Swedish Research Council (VR).

REFERENCES

- Adolfath, R. M., A. G. Petukhov, and I. Zutic, 2008, *Phys. Rev. Lett.* **101**, 207202.
- Ali, S., N. Shukla, and P. K. Shukla, 2007, *Europhys. Lett.* **78**, 45001.
- Ancona, M. G., and G. J. Iafrate, 1989, *Phys. Rev. B* **39**, 9536.
- Anderson, D., B. Hall, M. Lisak, and M. Marklund, 2002, *Phys. Rev. E* **65**, 046417.
- Andreev, A. V., 2000, *JETP Lett.* **72**, 238.
- Ang, L. K., T. J. T. Kwan, and Y. Y. Lau, 2003, *Phys. Rev. Lett.* **91**, 208303.
- Ang, L. K., and P. Zhang, 2007, *Phys. Rev. Lett.* **98**, 164802.
- Atwater, H. A., 2007, *Sci. Am.* **296**, 56.
- Azechi, H., *et al.*, 2006, *Plasma Phys. Controlled Fusion* **48**, B267.
- Balescu, R., and W. Zhang, 2009, *J. Plasma Phys.* **40**, 215.
- Barnes, W., A. Dereux, and T. Ebbesen, 2003, *Nature (London)* **424**, 824.
- Baym, G., and L. P. Kadanoff, 1961, *Phys. Rev.* **124**, 287.
- Becker, K. H., K. H. Schoenbach, and J. G. Eden, 2006, *J. Phys. D* **39**, R55.
- Benvenuto, O. G., and M. A. De Vito, 2005, *Mon. Not. R. Astron. Soc.* **362**, 891.
- Berestetskii, B., E. M. Lifshitz, and L. P. Pitaevskii, 1999, *Quantum Electrodynamics* (Butterworth-Heinemann, Oxford), p. 123.
- Bohm, D., 1953, *Phys. Rev.* **92**, 626.
- Bohm, D., and D. Pines, 1953, *Phys. Rev.* **92**, 609.

- Bonitz, M., 1998, *Quantum Kinetic Theory* (Teubner, Stuttgart).
- Bransden, B.H., and C.J. Joachain, 2000, *Quantum Mechanics* (Pearson Education Limited, Essex, England), 2nd ed.
- Brittin, W.E., and W.R. Chappell, 1962, *Rev. Mod. Phys.* **34**, 620.
- Brodin, G., and M. Marklund, 2007a, *New J. Phys.* **9**, 277.
- Brodin, G., and M. Marklund, 2007b, *Phys. Plasmas* **14**, 112107.
- Brodin, G., and M. Marklund, 2007c, *Phys. Rev. E* **76**, 055403(R).
- Brodin, G., M. Marklund, and G. Manfredi, 2008a, *Phys. Rev. Lett.* **100**, 175001.
- Brodin, G., M. Marklund, J. Zamanian, A. Ericsson, and P.L. Mana, 2008b, *Phys. Rev. Lett.* **101**, 245002.
- Brodin, G., A.P. Misra, and M. Marklund, 2010, *Phys. Rev. Lett.* **105**, 105004.
- Burt, P., and D. Wahlquist, 1962, *Phys. Rev.* **125**, 1785.
- Carruthers, P., and F. Zachariasen, 1983, *Rev. Mod. Phys.* **55**, 245.
- Chabrier, G., 2009, *Plasma Phys. Controlled Fusion* **51**, 124014.
- Chabrier, G., D. Saumon, and A.Y. Potekhin, 2006, *J. Phys. A* **39**, 4411.
- Chabrier, G., *et al.*, 2002, *J. Phys. Condens. Matter* **14**, 9133.
- Chandrasekhar, S., 1931a, *Astrophys. J.* **74**, 81.
- Chandrasekhar, S., 1931b, *Philos. Mag.* **11**, 592.
- Chandrasekhar, S., 1935, *Mon. Not. R. Astron. Soc.* **95**, 207.
- Chandrasekhar, S., 1939, *An Introduction to the Study of Stellar Structure* (University of Chicago Press, Chicago), p. 360.
- Chang, D.E., A.S. Sørensen, P.R. Hemmer, and M.D. Lukin, 2006, *Phys. Rev. Lett.* **97**, 053002.
- Chen, F.F., 2006, *Introduction to Plasma Physics and Controlled Fusion. Volume 1, Plasma Physics*. (Springer, New York), 2nd ed.
- Coe, M.J., A.R. Engel, and J.J. Quenby, 1978, *Nature (London)* **272**, 37.
- Cowley, S.C., R.M. Kulsrud, and E. Valeo, 1986, *Phys. Fluids* **29**, 430.
- Crouseilles, N., P.A. Hervieux, and G. Manfredi, 2008, *Phys. Rev. B* **78**, 155412.
- de Groot, S.R., and L.G. Suttrop, 1972, *Foundations of Electrodynamics* (North-Holland, Amsterdam).
- Dharma-wardana, C., and F. Perrot, 1995, in *Density Functional Theory*, edited by E.K.U. Gross, and R.M. Dreizler (Plenum Press, New York).
- Dirac, P.A.M., 1981, *Principles of Quantum Mechanics* (Oxford University Press, Oxford).
- Doms, A., P.-G. Reinhard, and E. Suraud, 1997, *Ann. Phys. (N.Y.)* **260**, 171.
- Drake, R.P., 2009, *Phys. Plasmas* **16**, 055501.
- Drake, R.P., 2010, *Phys. Today* **63**, 28.
- Egger, R., W. Häusler, C.H. Mak, and H. Grabert, 1999, *Phys. Rev. Lett.* **82**, 3320.
- Eliasson, B., and P.K. Shukla, 2008a, *J. Plasma Phys.* **74**, 581.
- Eliasson, B., and P.K. Shukla, 2008b, *Phys. Plasmas* **15**, 102102.
- Eliezer, S., P. Norreys, J.T. Mendonça, and K. Lancaster, 2005, *Phys. Plasmas* **12**, 052115.
- Else, D., R. Kompaneets, and S.V. Vladimirov, 2010, *Phys. Rev. E* **82**, 026410.
- Ferry, D.K., and J.-R. Zhou, 1993, *Phys. Rev. B* **48**, 7944.
- Feynman, R.P., and H. Kleinert, 1986, *Phys. Rev. A* **34**, 5080.
- Filinov, A.V., M. Bonitz, and Yu.E. Lozovik, 2001, *Phys. Rev. Lett.* **86**, 3851.
- Fortov, V.E., 2009, *Phys. Usp.* **52**, 615.
- Frisch, U., 1995, *Turbulence* (Cambridge University Press, Cambridge).
- Froula, D.H., S.H. Glenzer, N.C. Luhmann, Jr., and J. Sheffield, 2011, *Plasma Scattering of Electromagnetic Radiation: Theory and Measurement Techniques* (Academic Press, New York), 2nd ed.
- Garcia, L.G., F. Haas, L.P.L. de Oliveira, and J. Goedert, 2005, *Phys. Plasmas* **12**, 012302.
- Gardner, C.L., and C. Ringhofer, 1996, *Phys. Rev. E* **53**, 157.
- Ghoshal, A., and Y.K. Ho, 2009a, *Phys. Rev. A* **79**, 062514.
- Ghoshal, A., and Y.K. Ho, 2009b, *J. Phys. B* **42**, 175006.
- Glenzer, S.H., and R. Redmer, 2009, *Rev. Mod. Phys.* **81**, 1625.
- Glenzer, S.H., *et al.*, 2007, *Phys. Rev. Lett.* **98**, 065002.
- Gregori, G., and D.O. Gericke, 2009, *Phys. Plasmas* **16**, 056306.
- Guillot, T., 1999, *Science* **286**, 72.
- Gursky, H., 1976, in *Frontiers of Astrophysics*, edited by E.H. Avrett (Harvard University Press, Cambridge, Massachusetts), Chap. 5, pp. 152,153.
- Haas, F., 2005, *Phys. Plasmas* **12**, 062117.
- Haas, F., 2007, *Europhys. Lett.* **77**, 45004.
- Haas, F., L.G. Garcia, J. Goedert, and G. Manfredi, 2003, *Phys. Plasmas* **10**, 3858.
- Haas, F., G. Manfredi, and M.R. Feix, 2000, *Phys. Rev. E* **62**, 2763.
- Haas, F., and P.K. Shukla, 2009, *Phys. Rev. E* **79**, 066402.
- Haas, F., J. Zamanian, M. Marklund, and G. Brodin, 2010, *New J. Phys.* **12**, 073027.
- Harding, A.K., and D. Lai, 2006, *Rep. Prog. Phys.* **69**, 2631.
- Haug, H., and A.-P. Jauho, 2007, *Quantum Kinetics in Transport and Optics of Semiconductors*, Springer Series in Solid-State Sciences No. 123 (Springer, Berlin).
- Haug, H., and S.W. Koch, 2004, *Quantum Theory of Optical and Electronic Properties of Semiconductors* (World Scientific, Singapore).
- Hillery, M., *et al.*, 1984, *Phys. Rep.* **106**, 121.
- Hohenberg, P., and W. Kohn, 1964, *Phys. Rev.* **136**, B864.
- Holland, P.R., 1993, *The Quantum Theory of Motion* (Cambridge University Press, Cambridge).
- Horn, H.M., 1991, *Science* **252**, 384.
- Hu, S.X., and C.H. Keitel, 1999, *Phys. Rev. Lett.* **83**, 4709.
- Hurley, K., *et al.*, 2005, *Nature (London)* **434**, 1098.
- Iafate, G.J., H.L. Grubin, and D.K. Ferry, 1981, *J. Phys. Colloques* **42**, C7-307.
- Ichimaru, S., 1982, *Rev. Mod. Phys.* **54**, 1017.
- Ichimaru, S., and S. Tanaka, 1986, *Phys. Rev. Lett.* **56**, 2815.
- Iroshnikov, P.S., 1964, *Sov. Astron.* **7**, 566.
- Jovanovic, D., and R. Fedele, 2007, *Phys. Lett. A* **364**, 304.
- Jüngel, A., D. Matthes, and J.F. Milisic, 2006, *SIAM J. Appl. Math.* **67**, 46.
- Karpman, V.I., and H. Washimi, 1977, *J. Plasma Phys.* **18**, 173.
- Kaw, P.K., and A. Sen, 1998, *Phys. Plasmas* **5**, 3552.
- Kelly, D.C., 1964, *Phys. Rev.* **134**, A641.
- Kittel, C., 1996 *Introduction to Solid State Physics* (John Wiley & Sons, Inc., New York), 7th ed.
- Kleinert, H., 1986, *Phys. Lett. B* **181**, 324.
- Klimontovich, Y.L., and V.P. Silin, 1952a, *Dokl. Akad. Nauk SSSR* **82**, 361.
- Klimontovich, Y.L., and V.P. Silin, 1952b, *Zh. Eksp. Teor. Fiz.* **23**, 151.
- Klimontovich, Y.L., and V.P. Silin, 1961, in *Plasma Physics*, edited by J.E. Drummond (McGraw Hill, New York), p. 35.
- Klitzing, K. v., G. Dorda, and M. Pepper, 1980, *Phys. Rev. Lett.* **45**, 494.
- Knight, B., and L. Sirovich, 1990, *Phys. Rev. Lett.* **65**, 1356.
- Koester, D., and G. Chanmugam, 1990, *Rep. Prog. Phys.* **53**, 837.
- Kohn W., and L.J. Sham, 1965, *Phys. Rev.* **140**, A1133.
- Kolmogorov, A.N., 1941a, *Dokl. Akad. Nauk SSSR* **30**, 301.
- Kolmogorov, A.N., 1941b, *Dokl. Akad. Nauk SSSR* **31**, 538.
- Kraichnan, R.H., 1965, *Phys. Fluids* **8**, 1385.
- Kremp, D., M. Schlanges, and W.D. Kraeft, 2005, *Quantum Statistics of Nonideal Plasmas* (Springer, Berlin).

- Kremp, D., Th. Bornath, M. Bonitz, and M. Schlanges, 1999, *Phys. Rev. E* **60**, 4725.
- Kritcher, A. L., *et al.*, 2008, *Science* **322**, 69.
- Kuzelev, M. V., and A. A. Rukhadze, 1999, *Phys. Usp.* **42**, 603.
- Kwong, N.-H., and M. Bonitz, 2000, *Phys. Rev. Lett.* **84**, 1768.
- Lai, D., 2001, *Rev. Mod. Phys.* **73**, 629.
- Landau, L. D., and E. M. Lifshitz, 1998a, *Quantum Mechanics* (Butterworth-Heinemann, Oxford).
- Landau, L. D., and E. M. Lifshitz, 1998b, *Statistical Physics* (Butterworth-Heinemann, Oxford).
- Lee, H. J., *et al.*, 2009, *Phys. Rev. Lett.* **102**, 115001.
- Lee, H. W., 1995, *Phys. Rep.* **259**, 147.
- Lesieur, M., 1990, *Turbulence in Fluids* (Kluwer, Dordrecht).
- Lifshitz, E. M., and L. P. Pitaevskii, 1981, *Physical Kinetics* (Butterworth-Heinemann, Oxford), p. 164.
- Lindhard, D. J., 1954, *K. Dan. Vidensk. Selsk. Mat. Fys. Medd.* **28**, 8.
- Lindl, J., 1995, *Phys. Plasmas* **2**, 3933.
- Lopreore, C. L., and R. E. Wyatt, 1999, *Phys. Rev. Lett.* **82**, 5190.
- Lundin, J., J. Zamanian, M. Marklund, and G. Brodin, 2007, *Phys. Plasmas* **14**, 062112.
- Maafa, N., 1993, *Phys. Scr.* **48**, 351.
- Madelung, E., 1927, *Z. Phys.* **40**, 322.
- Maier, S. A., 2007, *Plasmonics* (Springer, New York).
- Malkin, V. M., N. J. Fisch, and J. S. Wurtele, 2007, *Phys. Rev. E* **75**, 026404.
- Manfredi, G., 2005, *Fields Inst. Commun.* **46**, 263.
- Manfredi, G., and F. Haas, 2001, *Phys. Rev. B* **64**, 075316.
- Manfredi, G., and P.-A. Hervieux, 2007, *Appl. Phys. Lett.* **91**, 061108.
- Marburger, J. H., and R. F. Tooper, 1975, *Phys. Rev. Lett.* **35**, 1001.
- Marklund, M., and G. Brodin, 2007, *Phys. Rev. Lett.* **98**, 025001.
- Marklund, M., G. Brodin, L. Stenflo, and C. S. Liu, 2008, *Europhys. Lett.* **84**, 17006.
- Marklund, M., and P. K. Shukla, 2006, *Rev. Mod. Phys.* **78**, 591.
- Markowich, P. A., *et al.*, 1990, *Semiconductor Equations* (Springer, Berlin).
- Masood, W., B. Eliasson, and P. K. Shukla, 2010, *Phys. Rev. E* **81**, 066401.
- Mayor, F. S., A. Askar, and H. A. Rabitz, 1999, *J. Chem. Phys.* **111**, 2423.
- McKinstrie, C. J., and R. Bingham, 1992, *Phys. Fluids B* **4**, 2626.
- Melrose, D. B., 2008, *Quantum Plasmadynamics: Unmagnetized Plasmas*, Lecture Notes Phys. No. 735 (Springer, New York).
- Melrose, D. B., and A. Mushtaq, 2009, *Phys. Plasmas* **16**, 094508.
- Mendonça, J. T., 2001, *Theory of Photon Acceleration* (Institute of Physics, Bristol).
- Misra, A. P., 2007, *Phys. Plasmas* **14**, 064501.
- Misra, A. P., 2009, *Phys. Plasmas* **16**, 033702.
- Misra, A. P., D. Ghosh, and A. R. Chowdhury, 2008, *Phys. Lett. A* **372**, 1469.
- Misra, A. P., and S. Samanta, 2010, *Phys. Rev. E* **82**, 037401.
- Mithen, J. P., J. Daligault, and G. Gregori, 2011, *Phys. Rev. E* **83**, 015401(R).
- Moyal, J. E., 1949, *Proc. Cambridge Philos. Soc.* **45**, 99.
- Murillo, M. S., 2010, *Phys. Rev. E* **81**, 036403 (2010).
- Murtaza, G. M., and P. K. Shukla, 1984, *J. Plasma Phys.* **31**, 423.
- Mushtaq, A., and D. B. Melrose, 2009, *Phys. Plasmas* **16**, 102110.
- National Research Council, 1995, *Plasma Science: From Fundamental Research to Technological Applications* (National Academy Press, Washington D.C.).
- Neumayer, P., *et al.*, 2010, *Phys. Rev. Lett.* **105**, 075003.
- Norreys, P. A., *et al.*, 2009, *Phys. Plasmas* **16**, 041002.
- Oberman, C., and A. Ron, 1963, *Phys. Rev.* **130**, 1291.
- Opher, M., *et al.*, 2001, *Phys. Plasmas* **8**, 2454.
- Ozbay, E., 2006, *Science* **311**, 189.
- Pines, D., 1961, *J. Nucl. Energy, Part C* **2**, 5.
- Pines, D., 1983, *Elementary Excitations in Solids* (Benjamin, Massachusetts).
- Pines, D., and P. Nozieres, 1989, *The Theory of Quantum Liquids* (Benjamin, New York).
- Redmer, R., and G. Röpke, 2010, *Contrib. Plasma Phys.* **50**, 970.
- Runge, E., and E. K. U. Gross, 1984, *Phys. Rev. Lett.* **52**, 997.
- Salamin Y. A., *et al.*, 2006, *Phys. Rep.* **427**, 41.
- Saleem, H., A. Ahmad, and S. A. Khan, 2008, *Phys. Plasmas* **15**, 014503.
- Serbeto, A., J. T. Mendonça, K. H. Tsui, and R. Bonifacio, 2008, *Phys. Plasmas* **15**, 013110).
- Serbeto, A., L. F. Monteiro, K. H. Tsui, and J. T. Mendonça, 2009, *Plasma Phys. Controlled Fusion* **51**, 124024.
- Serimaa, O. T., J. Javanainen, and S. Varro, 1986, *Phys. Rev. A* **33**, 2913.
- Shaikh, D., and P. K. Shukla, 2007, *Phys. Rev. Lett.* **99**, 125002.
- Shaikh, D., and P. K. Shukla, 2008, *New J. Phys.* **10**, 083007.
- Shapiro, S. L., and S. L. Teukolsky, 1983, *Black Holes, White Dwarfs, and Neutron Stars: The Physics of Compact Objects* (John Wiley & Sons, New York).
- Sharma, R. P., and P. K. Shukla, 1983, *Phys. Fluids* **26**, 87.
- Shokri, B., and A. A. Rukhadze, 1999, *Phys. Plasmas* **6**, 3450.
- Shpatakovskaya, G., 2006, *J. Exp. Theor. Phys.* **102**, 466.
- Shukla, P. K., 2006, *Phys. Lett. A* **352**, 242.
- Shukla, P. K., 2007, *Phys. Lett. A* **369**, 312.
- Shukla, P. K., 2009, *Nature Phys.* **5**, 92.
- Shukla, P. K., and B. Eliasson, 2006, *Phys. Rev. Lett.* **96**, 245001.
- Shukla, P. K., and B. Eliasson, 2007, *Phys. Rev. Lett.* **99**, 096401.
- Shukla, P. K., and B. Eliasson, 2008b, *Phys. Rev. Lett.* **100**, 036801.
- Shukla, P. K., and B. Eliasson, 2010, *Phys. Usp.* **53**, 51.
- Shukla, P. K., N. N. Rao, M. Y. Yu, and N. L. Tsintsadze, 1986, *Phys. Rep.* **138**, 1.
- Shukla, P. K., and L. Stenflo, 2006, *Phys. Plasmas* **13**, 044505.
- Shukla, P. K., and M. Y. Yu, 1984, *Plasma Phys. Controlled Fusion* **26**, 841.
- Shukla, P. K., M. Y. Yu, H. U. Rahman, and K. H. Spatschek, 1981, *Phys. Rev. A* **23**, 321.
- Silin, V. P., and A. A. Rukhadze, 1961, *Electromagnetic Properties of Plasmas and Plasma-like Media* (Gosatomizdat, Moscow).
- Simpson, G., C. Sulem, and P. L. Sulem, 2009, *Phys. Rev. E* **80**, 056405.
- Son, S., and N. J. Fisch, 2005, *Phys. Rev. Lett.* **95**, 225002.
- Steinberg, M., 2000, *Thermodynamics and Kinetics of a Magnetized Quantum Plasma* (Logos, Berlin).
- Stenflo, L., and P. K. Shukla, 2009, in *From Leonardo to ITER: Nonlinear and Coherence Aspects*, edited by J. Weiland, AIP Conf. Proc. No. 1177 (AIP, New York), p. 4.
- Stockman, M. I., 2011, *Phys. Today* **64**, 39.
- Stratonovich, R. L., 1956, *Sov. Phys. Dokl.* **1**, 414.
- Takabayasi, T., 1955, *Prog. Theor. Phys.* **14**, 283.
- Thiele, R., T. Bornath, C. Fortmann, A. Höll, R. Redmer, H. Reinholz, G. Röpke, A. Wierling, S. H. Glenzer, and G. Gregori, 2008, *Phys. Rev. E* **78**, 026411.
- Tsintsadze, L. N., 2010, in *New Frontiers in Advanced Plasma Physics*, edited by B. Eliasson and P. K. Shukla, AIP Conf. Proc. No. 1306 (AIP, New York), p. 89.
- Tsintsadze, N. L., and L. N. Tsintsadze, 2009, *Europhys. Lett.* **88**, 35001.

- Watanabe, H., 1956, *J. Phys. Soc. Jpn.* **11**, 112.
- Wigner, E., 1932, *Phys. Rev.* **40**, 749.
- Wilhelm, H.E., 1971, *Z. Phys.* **241**, 1.
- Wyatt, R.E., 2005, *Quantum Dynamics with Trajectories: Introduction to Quantum Hydrodynamics* (Springer Science, New York).
- Xia, S. X., W.C. Hua, and G. Feng, 2010, *Chin. Phys. Lett.* **27**, 025204.
- Yu, M. Y., *et al.*, 1974, *Z. Naturforsch. A* **29**, 1736.
- Zamanian, J., M. Marklund, and G. Brodin, 2010, *New J. Phys.* **12**, 043019.
- Zhang, W., and R. Balescu, 1988, *J. Plasma Phys.* **40**, 199.